Combinatorial Wnt signaling landscape during brachiopod anteroposterior patterning

Bruno C. Vellutini[1,2,*] José M. Martín-Durán[1,3] Aina Børve[1,4]
Andreas Hejnol[1,4,5,*]

[1] Michael Sars Centre, University of Bergen, Thormøhlensgate 55, 5008 Bergen, Norway.

[2] Max Planck Institute of Molecular Cell Biology and Genetics, Pfotenhauerstraße 108, 01307 Dresden, Germany.

[3] Queen Mary University of London, School of Biological and Behavioural Sciences, Mile End Road, Fogg Building, E1 4NS London, UK

[4] Department of Biological Sciences, Molecular Biology, University of Bergen, Thormøhlensgate 55, 5008 Bergen, Norway.

[5] Institute of Zoology and Evolutionary Research, Friedrich Schiller University Jena, Erbertstraße 1, 07743 Jena, Germany

[*] Correspondence: Bruno C. Vellutini <vellutini@mpi-cbg.de>, Andreas Hejnol <andreas.hejnol@uib.no>

Abstract

Background: Wnt signaling pathways play crucial roles in animal development. They establish embryonic axes, specify cell fates, and regulate tissue morphogenesis from the early embryo to organogenesis. It is becoming increasingly recognized that these distinct developmental outcomes depend upon dynamic interactions between multiple ligands, receptors, antagonists, and other pathway modulators, consolidating the view that a combinatorial "code" controls the output of Wnt signaling. However, due to the lack of comprehensive analyses of Wnt components in several animal groups, it remains unclear if specific combinations always give rise to specific outcomes, and if these combinatorial patterns are conserved throughout evolution.

Results: In this work, we investigate the combinatorial expression of Wnt signaling components during the axial patterning of the brachiopod *Terebratalia transversa*. We find that *T. transversa* has a conserved repertoire of ligands, receptors, and antagonists. These genes are expressed throughout embryogenesis but undergo significant upregulation during axial elongation. At this stage, Frizzled

domains occupy broad regions across the body while Wnt domains are narrower and distributed in partially overlapping patches; antagonists are mostly restricted to the anterior end. Based on their combinatorial expression, we identify a series of unique transcriptional subregions along the anteroposterior axis that coincide with the different morphological subdivisions of the brachiopod larval body. When comparing these data across the animal phylogeny, we find that the expression of Frizzled genes is relatively conserved, whereas the expression of Wnt genes is more variable.

Conclusions: Our results suggest that the differential activation of Wnt signaling pathways may play a role in regionalizing the anteroposterior axis of brachiopod larvae. More generally, our analyses suggest that changes in the receptor context of Wnt ligands may act as a mechanism for the evolution and diversification of the body axis of bilaterians.

Keywords

Brachiopoda, Gene expression, Axial patterning, Wnt pathways, Larva, Combinatorial regulation, Receptor context

Background

Wnt genes play multiple roles during embryogenesis [1]. They are involved in cell specification events, such as mediating cell fate decisions in early embryos [2–4], specifying endomesodermal tissues before gastrulation [5–9], and establishing the primary embryonic axis [10, 11]—often acting as a symmetry-breaking signal [12]. But Wnt activity also controls morphogenetic movements, such as apical constriction, convergent extension, and cell migration [13–19]. This multitude of roles is linked to the outstanding complexity of Wnt signaling pathways. There are 13 subfamilies of Wnt ligands, five subfamilies of Frizzled receptors, some additional co-receptors, as well as a series of agonists, antagonists, downstream players, and effector molecules that are involved in at least three interconnected Wnt pathways. The Wnt/beta-catenin (canonical) pathway regulates cell fate specification through the activity of beta-catenin, the Wnt/PCP (planar cell polarity) pathway controls cell polarity during tissue morphogenesis, and the Wnt/calcium pathway regulates intracellular calcium levels for convergent extension movements [20]. Therefore, understanding how this complex network of interactions regulates embryonic development and influences developmental evolution remains a major challenge.

The discovery of staggered Wnt expression domains in the tail bud of amphioxus embryos [21] and along the body axis of sea anemone embryos [22] raised the hypothesis that different combinations of Wnt genes can pattern different body regions. This idea, commonly referred to as the *Wnt code* or *landscape* [23–25], is an analogy to the *Hox code*, where the combinatorial expression of nested

Hox domains determines the positional identities of tissues along the body axis [26]. Over the years, however, it has been increasingly recognized that the output of Wnt signaling does not depend solely on the expression of Wnt ligands. In fact, Wnt pathways operate via an intricate network of dynamic protein interactions where the downstream response depends on the local availability of receptors, the presence of different antagonists, and the activity of pathway modulators [27, 28]. That means that, depending on the receptors present in the tissue, one Wnt ligand can activate or inhibit a different Wnt pathway and thus determine processes as diverse as fate specification, cellular organization, and tissue morphogenesis [29–31]. This complexity makes the Wnt code particularly challenging to elucidate.

A necessary step to untangle this combinatorial code is to extend the analyses of ligand–receptor contexts of Wnt genes to other animal groups using a comparative approach [32]. The comparison between flies and other animals was crucial to reveal the broader importance of the Hox genes as a high-level axial patterning system and not merely an arthropod-specific feature linked to body segmentation [33–35]. But while the expression of some Wnt genes is conserved in different animals (e.g., *wnt8* is expressed in the neuroectoderm of vertebrates [36, 37] and in spiders [25], annelids [38], and hemichordates [39]), it remains unclear if the organization of Wnt domains along the embryonic body axis and their combinatorial expression with other pathway components is conserved across the animal phylogeny.

While the expression of Wnt ligands has been widely studied in vertebrates and ecdysozoans [40], the receptor-context information is often lacking in several animal groups. Fewer works have analyzed the Wnt signaling in the Spiralia, a major branch of bilaterian animals with a great diversity of body patterns [41, 42]. In contrast to ecdysozoans which have lost several Wnt genes [43–45], the spiralians have retained the ancestral Wnt complement [25, 46, 47], indicating that they can be an informative group to understand the role of Wnt signaling in axial patterning evolution. However, most analyses about Wnt genes in Spiralia were performed in a few typical lineages, such as annelids and mollusks, and less is known about Wnt genes in other spiralians, which makes it difficult to reconstruct the ancestral state for this large animal group.

Brachiopods are sessile spiralians with bivalve shells [48]. They have a reduced adult morphology, but an outstanding embryonic development where a radially symmetric gastrula undergoes a series of morphogenetic changes to form a larval body subdivided into a series of distinct lobes along the anteroposterior axis [49, 50]. In previous studies using the rhynchonelliform brachiopod *Terebratalia transversa* (Sowerby, 1846)—whose embryogenesis and fate map are well-characterized [51–55]—we found that Wnt signaling plays a role in the specification of the endomesoderm and posterior fates [56], and in the patterning of the head–trunk boundary [57]. Moreover, we found that over-activation

of the Wnt/beta-catenin pathway disrupts the molecular and morphological organization of the larval subdivisions [56, 57], suggesting that Wnt activity contributes to the axial patterning of the larva. However, a full characterization of the Wnt signaling components and their developmental expression, including the ligand–receptor contexts is lacking for *T. transversa*, and for brachiopods in general.

In this study, we characterize the Wnt complement of the brachiopod *T. transversa* and investigate the spatiotemporal expression of Wnt signaling components throughout embryogenesis. We find that during axial elongation, the expression of ligands, receptors, and antagonists show an anteroposterior organization forming regionalized transcriptional territories, each expressing a unique combination of transcripts. These territories precede and coincide with the morphological subdivisions of the larval body, indicating that the differential activation of Wnt signaling may contribute to pattern the brachiopod larval body. We identified differences in receptor-context that may be involved in patterning an evolutionary novelty of lecithotrophic brachiopod larvae, the reversible mantle lobe. A comparative analysis reveals that while the expression of Frizzled receptors is evolutionarily conserved, the expression of Wnt ligands is more variable. This suggests that the evolutionary shuffling in the expression of Wnt ligands may be a mechanism underlying the evolution of anteroposterior diversification in bilaterians.

Results

Terebratalia transversa has a conserved repertoire of Wnt genes

Wnt genes encode secreted glycoproteins with a conserved series of cysteine residues [58]. Metazoans have a large Wnt repertoire with 13 subfamilies [22, 47, 59]. To characterize the Wnt complement of the brachiopod *Terebratalia transversa*, we surveyed our transcriptomic and genomic resources for Wnt genes using similarity searches with known Wnt genes from other animals. We identified 13 Wnt genes with representatives of 12 of the 13 Wnt subfamilies (Figure 1). *T. transversa* is missing *wnt3*, a gene known to have been lost in Protostomia [25, 47], and has two copies of *wnt1*. One of the *wnt1* paralogs—named hereafter *wnt1t*—is highly divergent at the sequence level compared to other *wnt1* orthologs across bilaterians, and our phylogenetic analysis suggests it originated via a lineage-specific duplication within *T. transversa* or rhynchonelliform brachiopods (Figure S1). Besides the loss of *wnt3* and duplication of *wnt1*, *T. transversa* shows a single representative ortholog for the remaining subfamilies, suggesting that the ancestral repertoire of metazoan Wnt genes remained largely conserved.

Wnt genes are upregulated in concert during axial elongation

To characterize the developmental dynamics of Wnt expression in *T. transversa*, we analyzed stage-specific RNA-seq data from the unfertilized egg to the post-metamorphic juveniles. We detect an abundance of *wnt4* and *wntA* transcripts deposited maternally in the oocyte (Figure 2). Transcripts of other Wnt genes, such as *wnt1t* and *wnt6*, are present at lower levels. This expression profile remains unchanged after fertilization (mid blastula, 8h) but shifts significantly at the late blastula stage (19h), when a concerted upregulation of *wnt1*, *wnt8*, *wnt10*, and *wnt16* occurs (Figure 2). Throughout gastrulation, Wnt genes continue to be upregulated with *wnt1* and *wnt5* in the early gastrula (26h); *wnt6*, *wnt7*, and *wnt11* in the mid gastrula (37h); and *wnt2*, *wnt9*, and *wnt10* in the late gastrula (51h). All Wnt genes are expressed between the late gastrula and early larva stages. Some, however, are downregulated after gastrulation (*wnt6* and *wnt10*) and after metamorphosis (*wnt7* and *wnt16*) (Figure 2). Therefore, Wnt expression is dynamic throughout development but peaks late in gastrulation, when the body elongates along the anteroposterior axis and at the onset of the morphological differentiation of the larval lobes in *T. transversa*.

Wnt domains partially overlap along the anteroposterior axis

To uncover the spatial localization of Wnt ligands during brachiopod development, we performed *in situ* hybridization in embryos from early gastrula to late larval stages of *T. transversa* (Figure 3 and 4).

wnt1 is expressed at the posterior lip of the blastopore in gastrula stages (Figure 3, Figure S2, and [57]). This domain expands laterally, forming a broad posterior ventral band of *wnt1* expression in the early larva, which encircles a subdivision of the pedicle lobe in subsequent stages. From the late gastrula stage, *wnt1* is also expressed anteriorly in a narrow stripe around the posterior region of the apical lobe and the dorsal shell primordium (Figure 3, Figure S2, and [57]).

wnt1t expression domains differ significantly from its paralog. We detect *wnt1t* transcripts in a single apical spot on the dorsal region of the gastrula stages (Figure 3 and Figure S2). This single spot becomes fragmented into bilateral domains in the early larva, which disappear in the late larva. Three novel *wnt1t* domains appear in larval stages, a central patch of ventral tissue posterior to the mouth, a ring domain beneath the mantle lobe, and a posterior spot in the terminal tip of the pedicle lobe (Figure 3 and Figure S2).

wnt2 is only expressed in the late gastrula and early larva stages. Broad bilateral bands encircle the posterior portion of the apical lobe almost entirely, and only the ventral and dorsal midlines are cleared from *wnt2* expression (Figure 3 and Figure S2).

wnt4 is expressed at the posterior end of the embryo during gastrula stages and acquires a subterminal

position within the pedicle lobe (Figure 3 and Figure S2). The pattern is similar to *wnt1*, but *wnt4* transcripts are localized more dorsally (Figure S3A–C).

wnt5 is expressed in three distinct domains—in the apical, mantle, and pedicle lobes, respectively. In the early gastrula, *wnt5* transcripts line the posterior blastopore lip in a band narrower than the *wnt1* domain (Figure 3 and Figure 5A). This posterior domain maintains a terminal position until the late larva stage when the tip of the pedicle lobe is cleared (Figure 3 and Figure S2). *wnt5* is also expressed in broad territories around the apical and mantle lobes from mid gastrula to early larva (Figure 3 and Figure S2). While the apical lobe domain fades in the late larva, the mantle lobe expression of *wnt5* remains strong on the leading edge of the growing mantle tissue (Figure 3 and Figure S2). The expression domains of *wnt5* and *wnt1* occupy distinct regions along the anteroposterior axis that coincide with the subdivisions of the larval lobes (Figure 5B,C and Figure S3G).

wnt6 transcripts localize to the posterior blastopore lip until the late gastrula stage (Figure 3 and Figure S2). This domain is cleared in the early larva stage, and *wnt6* is activated in the mid-body endoderm (Figure 3 and Figure S2). In the late larva, we also detect *wnt6* expression in the apical and pedicle lobes (Figure 3).

wnt7 initiates as a lateral pair of anterior stripes that progressively extend around the entire embryo circumference in the early larva stage (Figure 3 and Figure S2). This *wnt7* stripe demarcates the apical–mantle boundary and overlaps with *engrailed*-expressing cells at the anteriormost region of the mantle lobe (Figure 5G,H and Figure S3I; see also [57]). In the early larva, a posterior stripe of *wnt7* appears on the pedicle lobe demarcating another boundary, the subdivision of the pedicle lobe into subterminal and terminal regions. This stripe is positioned between the posterior territories of *wnt1* and *wnt5* in the pedicle lobe and partially overlaps with the *engrailed* domain (Figure 5G,H and Figure S3I).

wnt8 expression is broadly upregulated on the vegetal pole of the blastula stages (Figure 2 and Figure S2). At the gastrula stage, the transcripts are cleared from the anterior blastopore lip, and two distinct domains remain: a pair of broad lateral territories in the apical lobe, and a wide posterodorsal domain in the pedicle lobe (Figure 4 and Figure S2). While the posterior domain clears during gastrulation, the anterior territories expand ventrally and dorsally, encircling the apical lobe (Figure 4 and Figure S2). These anterior *wnt8* territories partially overlap with the anterior expression of *wnt1* (Figure 5I–L and Figure S3H).

wnt9 is initially detected in ventral cells internalized within the blastopore of late gastrula embryos (Figure 4 and Figure S2). They form a contiguous patch of mesodermal and endodermal cells expressing *wnt9* in the early larva. While the endodermal domain becomes elongated along the central portion of the gut, the mesodermal expression develops into a distinct bilateral pair of anterior domains (Figure 4

and Figure S2).

wnt10 is expressed in a posterior domain on the subterminal region of the pedicle lobe in gastrula and larval stages (Figure 4 and Figure S2).

wnt11 shows a terminal posterior domain during gastrulation that encircles the pedicle lobe in the early larva, and is reduced to a thin subterminal ventral stripe in the late larva (Figure 4 and Figure S2). We also detect *wnt11* in the central and posterior portions of the gut of the early larva stage (Figure 4 and Figure S2).

wnt16 is expressed in lateral patches around the blastopore. During gastrulation, blastopore closure brings these patches together, forming a heart-shaped domain in the midline of the early larva (Figure 4 and Figure S2). The *wnt16*-expressing cells localize to a central portion of the mantle lobe mesoderm (Figure 4 and Figure S2).

wntA appears in the late gastrula as paired ventral domains at the posterior portion of the apical lobe (Figure 4 and Figure S2). In the late larva, these anterior ectodermal domains are cleared, and *wntA* expression is activated in two anterior mesodermal bands next to the mouth (Figure 4 and Figure S2).

Overall, Wnt genes are expressed in diverse, partially overlapping domains along the anteroposterior axis.

Frizzled genes are highly expressed and show gradual changes throughout embryogenesis

Frizzled genes encode seven-pass transmembrane proteins with an extracellular cystein-rich domain and act as receptors in Wnt signaling pathways [60]. There are five Frizzled subfamilies in metazoans [61], but the subfamily *fz3/6* is only found in tunicates and vertebrates [62]. In the brachiopod *T. transversa*, we identified a total of four Frizzled genes with a single ortholog for the *fz1/2/7*, *fz5/8*, *fz9/10*, and *fz4* subfamilies, respectively (Figure S4).

Frizzled receptors are expressed throughout *T. transversa* development. In the unfertilized oocyte, *fz1/2/7* and *fz5/8* are highly expressed (Figure 2). The expression of *fz1/2/7* remains high from the oocyte to juvenile stages, while the expression of *fz5/8* peaks before gastrulation and decays over time. *fz4*, which is initially expressed at lower levels, peaks late in development, at the larval stages, an expression profile complementary to the one of *fz5/8* (Figure 2). In contrast, *fz9/10* expression increases during gastrulation and remains relatively constant in subsequent stages.

Overall, each Frizzled shows a unique expression profile but in contrast to Wnt dynamic changes, the levels of Frizzled transcripts change more gradually during development.

Frizzled domains occupy broad but distinct body regions

We carried out *in situ* hybridization for all Frizzled genes of *T. transversa* to reveal their domains of expression during axial elongation (Figure 6).

fz1/2/7 transcripts are almost ubiquitous in the tissues of gastrulating embryos (Figure 6). We observe an anteroposterior gradient with stronger signal at the apical region, in the anterior mesoderm, and in a pair of lateral ectodermal domains in the middle of the body (Figure 6 and Figure S5). The posterior transcripts are cleared from the pedicle lobe late in gastrulation but are up-regulated in the terminal portion of the pedicle lobe in the late larva, becoming nearly ubiquitous again (Figure 6).

fz4 is expressed in a subapical ectodermal ring encircling the animal pole from the early gastrula until the late larva stage (Figure 6 and Figure S5). The anterior portion of the mesoderm in the apical lobe also expresses *fz4* in all developmental stages (Figure 6 and Figure S5). From the late gastrula, we detect *fz4* in the dorsal ectoderm between the mantle and pedicle lobe. This domain becomes stronger in the late larva as it expands around the pedicle lobe and beneath the mantle lobe, including in the mantle mesoderm (Figure 6 and Figure S5). An additional *fz4* domain appears at the posterior tip of the pedicle lobe in the late larva (Figure 6 and Figure S5). The incremental appearance of *fz4* domains during development correlates with the increase in its expression in the RNA-seq data (Figure 2).

fz5/8 is expressed in the ectoderm of the apical cap from the early gastrula to the late larva (Figure 6 and Figure S5). This domain is complementary to the *fz4* domain in the apical lobe and does not overlap with the apical domain of *wnt5* (Figure 5E,F). We also detect *fz5/8* in a narrow portion of the anterior mesoderm and in the mesoderm of the chaetae sacs in the late larva stage (Figure 6 and Figure S5).

fz9/10 transcripts are present around the blastopore and animal pole of the early gastrula, but not at the apical cap (Figure 6 and Figure S5). The anterior limit of *fz9/10* expression coincides with the posteriormost portion of the apical lobe and abuts the *fz4* domain posteriorly. The posterior limit of *fz9/10* domain reaches the pedicle lobe, where it overlaps with *wnt1*. Mantle lobe expression is weak, and the terminal portion of the pedicle lobe is cleared from *fz9/10* transcripts (Figure 6 and Figure S5). Throughout development, *fz9/10* is also expressed in the mesoderm.

Taken together, the expression domains of Frizzled receptors extend over broad but distinct body regions, and their anteroposterior arrangement remains stable throughout gastrulation and larval morphogenesis.

Expression of Wnt antagonists is limited to the anterior end

To obtain a more comprehensive picture of the Wnt signaling landscape in *T. transversa*, we also analyzed the expression of three Wnt antagonist genes: a Secreted Frizzled-Related Protein (*sfrp*), a Dickkopf protein (*dkk*), and a Wnt Inhibitory Factor (*wif*).

sFRP is a soluble protein that antagonizes Wnt activity by directly binding to Wnt ligands or to Frizzled receptors [63]. It has a cysteine-rich domain with high-affinity to Wnt proteins. The sFRP family can be divided into two subfamilies, *sfrp1/2/5* and *sfrp3/4* [63, 64]. In *T. transversa*, we only identified a *sfrp1/2/5* ortholog (Figure S6). *sfrp1/2/5* is highly expressed throughout development (Figure 2). The transcripts are located in the anterior-most portion of the mesoderm and in the apical cap ectoderm—a pattern similar to the expression of *fz5/8* (Figure 6 and Figure S7). Transient mesodermal domains appear in the mantle lobe of the early larva but, except for dorsal patches on the apical lobe, the expression of *sfrp1/2/5* fades in the late larva stage (Figure 6 and Figure S7).

Dkk is a secreted glycoprotein containing two cysteine-rich domains that antagonizes Wnt signaling by inhibiting *lrp5/6* co-receptors [65, 66]. These proteins are generally divided into two subfamilies, *dkk1/2/4* and *dkk3* [65]. In *T. transversa*, however, we identified a single *dkk* ortholog that groups with a previously unidentified Dkk subfamily, named hereafter *dkk5* (Figure S8). Our phylogenetic analysis reveals that non-vertebrate deuterostomes, such as hemichordates and cephalochordates, have orthologs for *dkk1/2/4*, *dkk3*, and *dkk5*, suggesting this was the ancestral Dkk repertoire of bilaterians, and that *dkk1/2/4* and *dkk5* were subsequently lost in protostomes and vertebrates, respectively (Figure S8). The expression of *dkk5* in *T. transversa* is upregulated in the late blastula and downregulated in the juvenile (Figure 2). It localizes to an apical ectodermal domain similar to the expression of *sfrp1/2/5*, but the *dkk5* domain is narrower and does not extend completely to the dorsal side (Figure 6 and Figure S7).

Wif is another protein that inhibits Wnt activity by direct binding to Wnt proteins [67]. The protein has five EGF repeats and a typical WIF domain which is shared with RYK receptor tyrosine kinases [66, 67]. In *T. transversa*, we identified one *wif* ortholog (Figure S9). The expression levels are relatively low and somewhat stable throughout development, with a peak in the late gastrula (Figure 2). Unlike *sfrp1/2/5* and *dkk5*, *wif* is mainly expressed in mesodermal tissues throughout the analyzed developmental stages (Figure 6 and Figure S7).

Overall, the expression of the analyzed Wnt antagonist genes is restricted to the anterior portion of the ectoderm (*sfrp1/2/5* and *dkk5*), and to the mesoderm (*wif*), regions which coincide with the absence or limited expression of Wnt ligands.

Planar cell polarity genes are expressed in patches during axial elongation

Proper regulation of planar cell polarity (PCP) is crucial to guide morphogenetic processes, such as convergent extension, and to orient the formation of structures during development [68, 69]. We identified several core components of the PCP pathway in *T. transversa*. These include orthologs for *dishevelled* (*dsh*, also known as *dvl*), *diego* (*dgo*, also known as *ankrd6* or *diversin*), *prickle* (*pk*), *flamingo* (*fmi*, also known as *stan* or *celsr*), *strabismus* (*stbm*, also known as *vang* or *vangl*), as well as the downstream transducer *c-jun n-terminal kinase* (*jnk*). Then, we analyzed their expression between the early and late gastrula stages.

Dsh is a central regulator of the cell fate and the cell polarity Wnt pathways [70]. The protein has three conserved domains (DIX, PDZ, and DEP domains), and two conserved regions before and after the PDZ domain [71]. In *T. transversa*, we identified a single copy of *dsh* (Figure S10) which is highly expressed in every developmental stage (Figure S11). *dsh* transcripts localize to a narrow domain in the apical ectoderm and anterior mesoderm (Figure 7).

Dgo is a cytoplasmic protein containing 6–8 ankyrin repeat domains that suppresses Wnt/beta-catenin signaling and activates the Wnt/PCP pathway [72, 73]. We found a single *dgo* ortholog in *T. transversa* with six ankyrin repeats (Figure S12). The expression levels are relatively low compared to the other genes we analyzed in this study (Figure S11). However, we detect two pairs of dorsal domains in the late gastrula, one in the apical and another in the pedicle lobe (Figure 7).

Pk is a protein that contains a PET domain and three LIM domains [74] and competes with Dgo for Dsh binding [75]. We identified a single *pk* ortholog in *T. transversa* (Figure S13), which is highly expressed throughout development (Figure S11). In the early gastrula, *pk* transcripts are expressed in a small patch of tissue posterior to the blastopore (Figure 7). Then, *pk* is upregulated in the ventral ectoderm of the apical lobe as bilateral domains and in the ventral mesoderm of the mantle lobe (Figure 7).

Fmi is a seven-pass transmembrane cadherin that regulates cell polarity [76, 77]. In *T. transversa*, we identified one ortholog of *fmi* (Figure S14). It is expressed at every developmental stage, peaking around the late gastrula (Figure S11). *fmi* transcripts are present in most ectodermal tissues but show stronger signal on bilateral patches present in the apical lobe of the late gastrula (Figure 7).

Stbm is a four-pass transmembrane protein that forms a signaling complex with FMI [78, 79]. *Terebratalia transversa stbm* ortholog (Figure S15) is initially expressed in high levels, which gradually decay during development (Figure S11). It is ubiquitously expressed in the tissues of gastrulating embryos (Figure 7).

Jnk is a kinase that regulates epithelial metamorphosis and is a downstream transducer of the PCP

pathway [80]. The *jnk* ortholog in *T. transversa* (Figure S16) is highly expressed throughout the development (Figure S11) and ubiquitously expressed in the late gastrula, except for broad bilateral regions in the apical lobe (Figure 7).

In conclusion, *fmi* and *stbm* are expressed ubiquitously. In contrast, the other cell polarity genes *dsh*, *dgo*, *pk*, and *jnk*—a readout of the PCP pathway—are expressed in non-overlapping patches at different regions of the late gastrula stage of *T. transversa*, when the embryo is elongating.

Discussion

Our work characterizes the expression of Wnt signaling components during brachiopod development. We find that the brachiopod *T. transversa* has largely retained the ancestral repertoire of Wnt genes showing few duplications or losses, and that these genes are upregulated during mid to late gastrula, when the embryo elongates. At this stage, we identify six distinct transcriptional subregions along the anteroposterior axis of the embryo, each expressing a unique combination of ligands, receptors, and antagonists of Wnt signaling (Figure 8A, Table 1). Interestingly, these transcriptional subregions coincide with the morphological subdivisions of the larval body (Figure 8B), suggesting that a combinatorial Wnt signaling logic—a *Wnt code*—may play a role in regionalizing the brachiopod anteroposterior body axis. Below, we discuss the evidence for different ligand–receptor contexts during brachiopod axial patterning, how these Wnt transcriptional subregions compare across the phylogeny, and the evolutionary implications of these observations.

Wnt ligand–receptor contexts in brachiopod axial patterning

The apical lobe of *T. transversa* differentiates into two regions, a narrower anterior region that gives rise to the larval apical organ and neuropile [81], and a wider posterior region that gives rise to the crown of tentacles used for filter feeding known as the lophophore. We find that these two regions have different Wnt transcriptional profiles. The anterior region expresses Wnt antagonists and *fz5/8* but no Wnt ligands, while the posterior region expresses several Wnt ligands and *fz4* but no Wnt antagonist (Figure 8A). It is known that *fz5/8* consolidates the anterior neuroectoderm identity of the apical pole by activating the Wnt antagonists *sFRP* and *Dkk* and inhibiting Wnt/beta-catenin signaling [82, 83]. This region is also characterized by the expression of neural genes such as *foxq2* and *six3/6* [84–87]. In turn, *wnt8* establishes a posterior neuroectoderm identity that subdivides the anterior end by repressing the expression of *fz5/8* [82, 88–91]. These gene expression arrangements are well conserved in the anterior/aboral ends of other animals [82, 92]. Not only does *T. transversa* show the same arrangement between *fz5/8* and *wnt8*, but also expresses *six3/6* and *foxq2* at the anterior region

[93]. Therefore, these data suggest that a similar regulatory logic may control the subdivision of the apical lobe in a brachiopod larva.

The apical lobe ends with a deep epithelial fold located at the boundary with the mantle lobe (Figure 8B). Previously, we found that this apical–mantle interface is demarcated by a sharp transcriptional boundary between *wnt1* and the homeobox transcription factor *engrailed* (*en*) [57]. Our current study reveals that *wnt7* is also expressed at the apical–mantle interface, and that the entire invaginated area corresponds to a single transcriptional subregion expressing *fz9/10* (Figure 8A). In other animals, *wnt1*, *wnt7*, and *en* are expressed in a variety of compartment boundaries, such as the trunk segments of arthropods [25] and the mid–hindbrain boundary of vertebrates [94, 95]. Moreover, Wnt7 is also known to interact with Fz9 *in vitro* [96]. Therefore, our data in *T. transversa* suggests that *fz9/10* could mediate Wnt signaling events at this transcriptional subregion, possibly patterning the apical–mantle boundary of larval brachiopods.

The mantle lobe lies in the middle of the larval body (Figure 8B). During development, its tissues undergo dramatic growth, forming a posterior skirt-like structure that is then reversed anteriorly during metamorphosis [52]. This reversible mantle lobe is considered an evolutionary innovation of lecithotrophic brachiopod larvae [97]. Our study reveals that the mantle lobe has a peculiar transcriptional profile where only a single Wnt ligand and Frizzled receptor are expressed: *wnt5* and *fz1/2/7*. In other animals, *wnt5* regulates the convergence and extension of tissues during morphogenesis [12, 15, 16, 98], and it is a gene commonly expressed in tissue outgrowths such as the tail and limb buds of vertebrates [21, 99, 100]. This is usually controlled by Wnt/PCP pathway [14]. These observations suggest that the convergent extension of tissues is mediated by the Wnt/PCP pathway, raising a potential mechanism for the morphogenesis of the mantle lobe in brachiopods.

Interestingly, *wnt5* signaling is known to depend on the receptor context. It usually inhibits the Wnt/beta-catenin pathway, but in the presence of *fz4* it can activate it instead [30]. While *wnt5* and *fz1/2/7* are co-expressed in the mantle lobe, *wnt5* is co-expressed with *fz4* in the apical lobe (Figure 8A). While the mantle lobe undergoes tissue outgrowth, the apical lobe undergoes intense cell proliferation [56]. The fact that the same ligand, when co-expressed with a different receptor, correlates with different developmental outcomes suggests that receptor availability is important for differentially patterning these body regions. Wnt signaling in the apical lobe is presumably mediated by *fz4* via the Wnt/beta-catenin, while in the mantle lobe, it is presumably mediated by *fz1/2/7* via the Wnt/PCP pathway. Indeed, over-activation of the Wnt/beta-catenin pathway in *T. transversa* leads to an expansion of the apical lobe and an inhibition of the mantle lobe [56, 57], indicating that *wnt5* is probably associated with distinct receptor contexts in the apical and mantle lobes (Figure 8A). Therefore, it is

possible that the evolution of a reversible mantle lobe was associated with the activation of *wnt5* in a different receptor context, indicating that such context-switching could have a significant role in axial evolution.

Finally, we reach the other end of *T. transversa*, the pedicle lobe. It is subdivided into a wider anterior portion that gives rise to the posterior region of the adult body, and a narrower posterior portion that gives rise to the pedicle, the structure attaching the adult to the substrate [53]. We find that these two regions have distinct transcriptional profiles expressing a battery of different Wnt genes (Figure 8A). Most notably, though, is the finding that the posterior portion expresses no Frizzled genes (Figure 8A). Such a receptor-free zone also occurs at the posterior end of hemichordates, a region that is Wnt-insensitive, since its transcriptional profile is not altered when the Wnt/beta-catenin pathway is over-activated or suppressed [39]. Two observations suggest that the receptor-free posterior region of *T. transversa* might also be Wnt-insensitive. The first is that this region does not express *axin* [56], a readout of the Wnt/beta-catenin pathway [101]. The second is that the expression of posterior markers, such as *evx* and *cdx*, remains unchanged when the Wnt/beta-catenin is over-activated [56]. While further experiments are needed to test this hypothesis, this preliminary evidence indicates that a Wnt-insensitive region may be present at the posterior end of *T. transversa*, and that it may contribute to differentiating the pedicle lobe regions during larval morphogenesis of brachiopods.

Altogether, these observations support that the transcriptional subregions we identified in *T. transversa* may play a role in the regional specification of tissues along the anteroposterior axis of brachiopods. The finding that the same ligand can be expressed in subregions that undergo different developmental fates and morphogenetic processes also indicates that the local receptor-context matters for development and may have been associated with an evolutionary innovation of lecithotrophic brachiopod larvae—the reversible mantle lobe. These data raise the idea that changes in these Wnt transcriptional subregions may have been important for the evolution of the primary body axis in animals. We have already described a few similarities between the brachiopod expression patterns and other animals (e.g., neuroectoderm patterning). However, what the ancestral state was and how conserved these Wnt transcriptional subregions are across the phylogeny remain unclear.

Combinatorial Wnt landscape across the animal phylogeny

A comparison across the phylogeny reveals that the modern Wnt repertoire emerged earlier than bilateral symmetry, before the Cnidaria–Bilateria split (Figure 9A). Ctenophores—the probable sister group to all other animals[102]—have only four Wnt genes and two Frizzled genes [103]. Their embryonic expression is polarized with opposed domains of ligands and antagonists, and there is an incipient staggered expression around the mouth but no obvious transcriptional subregions along the body axis

[103]. In contrast, cnidarians and bilaterians have a much larger set of ligands, receptors, and antagonist genes expressed in staggered domains along the body axis (Figure 9A). These comparative data suggest an initial axial polarity role for Wnt signaling in early development. Only secondarily, with the expansion of the Wnt complement in the last common ancestor to Cnidaria and Bilateria, Wnts became involved in late axial patterning. Therefore, this role precedes the evolution and diversification of a bilaterally symmetric body with an anteroposterior axis [23].

Despite the great differences in embryo architecture, a broader comparison across the tree reveals a general common pattern for the expression of Wnt signaling components. Wnt antagonist genes are expressed anteriorly, while Wnt genes are predominantly not expressed anteriorly, and Frizzled genes are expressed along the entire body (Figure 9A). Frizzled domains are usually broad without much overlap, while Wnt domains are narrower and overlap with other Wnt genes. But what is most notable in this comparative overview is that the spatiotemporal expression of Frizzled genes is relatively well-conserved, while the expression of Wnt ligands is more variable between species (Figure 9A).

This pattern occurs for both the maternal load of Wnt signaling components and the later axial expression. For instance, the maternal load of Frizzled transcripts is highly conserved across animals, with most species showing *fz1/2/7* expression in the egg (Table 2) [104]. Accordingly, Frizzled expression domains follow the same anteroposterior arrangement in different animals with *fz5/8* in the head, *fz9/10* in the trunk, and *fz1/2/7* broadly expressed (Figure 8A, 9A and S17A). In fact, the spatial organization of Frizzled domains is almost identical between the brachiopod *T. transversa* and the hemichordate *Saccoglossus kowalevskii* (Figure S17A,B). In both cases, these broad domains coincide with their different body regions, suggesting that each receptor may regulate the regional patterning along the anteroposterior axis [39]. The only exception is *fz4*; its spatial localization is variable in other animals, such as cnidarians [105], echinoderms [106, 107] and cephalochordates [108]. The similarity in Frizzled expression indicates that this spatial organization is a shared, ancient feature that remained conserved within the Cnidaria–Bilateria clade during evolution.

In contrast, the spatiotemporal expression of Wnt genes during the axial patterning of different animals varies considerably. A comparison of the maternal load of Wnt ligands reveals that they are highly variable and can even differ between closely related species (Table 2). A similar picture occurs in the axial patterning: the spatiotemporal expression of most Wnt genes shows great variability (Figure 9A). One example is the expression of *wnt9* and *wnt11* which are expressed at the posterior end of the brachiopod but at the anterior end of the hemichordate in entirely different receptor contexts (Figure S17A). Accordingly, Wnt genes also show variable expression across the chordate lineage [109].

Only a few Wnt-Frizzled combinations are relatively conserved across bilaterians (9A,B). Therefore, these observations suggest that ligand exchange and re-deployment to different tissues and receptor contexts may have occurred more frequently during evolution than previously thought.

The variation in Wnt expression compared to the conservation of Frizzled expression may reflect an important feature of axial evolution. The ability of Wnt proteins to elicit different fate decisions and morphogenetic processes depending on the developmental context places Wnt signaling pathways as key players in generating cellular and tissue diversity in the body patterning of animals [12, 24]. Changes in the ligand–receptor context during evolution could effectively alter cell fates and morphogenetic events, providing a basis for the establishment of developmental innovations. We hypothesize that this evolutionary shuffling of Wnt ligands may be one key mechanism involved in the diversification of the body axis of animals.

Conclusions

In summary, we characterize the complement and expression of Wnt signaling components in a brachiopod. We find a strong correlation between transcriptional subregions and morphological subdivisions of the larval body with different morphogenesis and fates. Our findings suggest that the differential activation of Wnt signaling pathways through this combinatorial landscape may regionalize the anteroposterior axis of brachiopods. The data also raises the hypothesis that differences in the receptor context could be associated with the evolution of a morphogenetic innovation in the mantle lobe of larval brachiopods. A comparative analysis reveals that only a few of the unique combinatorial patterns we observe in the brachiopod occur in other animals, despite the widely conserved expression of Frizzled genes. This is because the expression of Wnt genes is variable. We propose that evolutionary changes in ligand–receptor context may have contributed to the diversification of the bilaterian anteroposterior axis. Investigating the combinatorial expression of Wnt components in a comparative way will be crucial to uncovering the multiple roles of an ever-changing Wnt landscape for the evolution of animals.

Methods

Sample collection

T. transversa (Sowerby, 1846) adult specimens were collected by dredging the rocky seabeds around Friday Harbor, San Juan Islands, USA. We kept in a seawater table with running seawater at the Friday Harbor Laboratories (University of Washington). To obtain embryos, we dissected the gonads of ripe

individuals and fertilized the gametes *in vitro* as previously described [55, 110]. We cultured the embryos in E-ware glass bowls (i.e., glassware never exposed to chemicals) with filtered seawater and temperature around 7.6 ℃. Water in culturing bowls was exchanged daily. Using a glass pipette, we collected samples for RNA sequencing and for *in situ* hybridization at representative developmental stages (Table 3). For the RNA-seq samples, we collected two biological replicates, each containing the eggs of a single female fertilized with mixed sperm from three different males. We preserved the embryos directly in RNAlater at room temperature. For the *in situ* hybridization samples, we fixed the embryos for 1h in 4% paraformaldehyde at room temperature, washed thoroughly in 1x PBS with 0.1% Tween-20, and stored them in 100% methanol at -20℃.

RNA sequencing and analyses

We extracted the total RNA using Trizol. Library preparation and sequencing was performed at the EMBL Genomic Core Facilities (GENECORE). The samples were randomized and multiplexed on four lanes of a Illumina HighSeq 2000 system, and sequenced to an average of 24±5 million 50bp of single-end reads. We quantified the transcript abundances by pseudoaligning the reads to a reference transcriptome of *T. transversa* (assembled from SRX1307070) using Kallisto v0.46.0 [111]. Using DESeq2 [112], we estimated the library size factors and data dispersion, and homogenized the variance across expression ranks applying a variance-stabilizing transformation before the expression analyses. We visualized the normalized expression data using pheatmap [113] and ggplot2 [114]. All analyses were performed in R [115] running RStudio Desktop [116].

Gene orthology

We searched for Wnt signaling orthologs in *T. transversa* by querying known sequences against the available transcriptome using BLAST+ [117]. To resolve the orthology of the obtained putative orthologs, we aligned the protein sequences of *T. transversa* with well-annotated proteins from other metazoans using MAFFT 7.310 [78], removed non-informative sections using GBlocks 0.91b [118], and inspected the multiple sequence alignment using UGENE [119]. Using the blocked alignments as input, we ran a maximum likelihood phylogenetic analysis using the automatic model recognition and rapid bootstrap options of RAxML 8.2.12 [120]. We rendered the resulting trees using the Interactive Tree Of Life web application [121].

Cloning and *in situ* hybridization

We synthesized cDNA from a mix of total RNA from all developmental stages using the SMARTer RACE cDNA Amplification kit (Clontech). For each identified ortholog transcript, we designed gene-

specific primer pairs within the coding sequence, with product sizes ranging between 800–1200bp, using Primer3 [122]. We cloned each fragment into a pGEM-T Easy Vector and amplified the antisense sequences using T7 or SP6 polymerase. DIG-labeled riboprobes were synthesized with the MEGAscript kit (Ambion). We then followed the established protocols in *T. transversa* for single colorimetric *in situ* hybridization [93, 123], and double fluorescent *in situ* hybridization [56, 57].

Microscopy and image processing

We mounted the embryos between a glass slide and a coverslip, supported by clay feet, in 70% glycerol in PBS. Using a Zeiss AxioCam HRc attached to a Zeiss Axioscope A1, we imaged the samples under differential interference contrast (DIC or Nomarski). For fluorescent samples, we scanned volumetric stacks in a Leica TCS SP5 confocal microscope and generated maximum intensity projections using Fiji [124]. We adjusted intensity levels without clipping high or low ranges to improve the contrast using Fiji or GIMP. Illustrations and figure plates were assembled using Inkscape.

Declarations

Availability of data and materials

The data and analyses are available in the Zenodo repository https://doi.org/10.5281/zenodo.8312023.

Competing interests

The authors declare that they have no competing interests.

Funding

The study was funded by the Michael Sars Centre core budget and by The European Research Council Community's Framework Program Horizon 2020 (2014–2020) ERC grant agreement 648861 to AH. The animal collections were supported by a Meltzer Research Fund. BCV was funded by an EMBO Long-Term Fellowship (ALTF 74-2018) during the writing of this manuscript.

Authors' contributions

AH, JMMD, and BCV designed the study and collected the samples. BCV, JMMD, and AB performed gene cloning, *in situ* hybridization, and imaging. BCV performed the phylogenetic and transcriptomic analyses. BCV analyzed the data, prepared the figures, and wrote the manuscript. AH and JMMD revised and contributed to the text. All authors read and approved the final manuscript.

Acknowledgments

We thank the Friday Harbor Laboratories boat crew for collecting the brachiopods, Yale Passamaneck for the help with spawnings, Katrine Worsaae for the initial gene cloning, and members of the Hejnol Lab for the helpful discussions. BCV thanks Pavel Tomančák for the generous support during the preparation of this work.

References

1. Cadigan KM, Nusse R. Wnt signaling: A common theme in animal development. Genes Dev. 1997;11:3286–305. doi:10.1101/gad.11.24.3286.

2. Goldstein B, Takeshita H, Mizumoto K, Sawa H. Wnt signals can function as positional cues in establishing cell polarity. Dev Cell. 2006;10:391–6. doi:10.1016/j.devcel.2005.12.016.

3. Schneider SQ, Bowerman B. β-catenin asymmetries after all animal/vegetal- oriented cell divisions in *Platynereis dumerilii* embryos mediate binary cell-fate specification. Dev Cell. 2007;13:73–86. doi:10.1016/j.devcel.2007.05.002.

4. Hudson C, Kawai N, Negishi T, Yasuo H. β-catenin-driven binary fate specification segregates germ layers in ascidian embryos. Curr Biol. 2013;23:491–5. doi:10.1016/j.cub.2013.02.005.

5. Logan CY, Miller JR, Ferkowicz MJ, McClay DR. Nuclear β-catenin is required to specify vegetal cell fates in the sea urchin embryo. Development. 1999;126:345–57. doi:10.1242/dev.126.2.345.

6. Imai K, Takada N, Satoh N, Satou Y. β-catenin mediates the specification of endoderm cells in ascidian embryos. Development. 2000;127:3009–20. doi:10.1242/dev.127.14.3009.

7. Henry JQ, Perry KJ, Wever J, Seaver E, Martindale MQ. β-catenin is required for the establishment of vegetal embryonic fates in the nemertean, *Cerebratulus lacteus*. Dev Biol. 2008;317:368–79. doi:10.1016/j.ydbio.2008.02.042.

8. Wikramanayake AH, Huang L, Klein WH. β-catenin is essential for patterning the maternally specified animal-vegetal axis in the sea urchin embryo. Proc Natl Acad Sci U S A. 1998;95:9343–8. doi:10.1073/pnas.95.16.9343.

9. Darras S, Gerhart J, Terasaki M, Kirschner M, Lowe CJ. β-catenin specifies the endomesoderm and defines the posterior organizer of the hemichordate *Saccoglossus kowalevskii*. Development. 2011;138:959–70. doi:10.1242/dev.059493.

10. Petersen CP, Reddien PW. Wnt signaling and the polarity of the primary body axis. Cell. 2009;139:1056–68. doi:10.1016/j.cell.2009.11.035.

11. Niehrs C. On growth and form: A Cartesian coordinate system of Wnt and BMP signaling specifies bilaterian body axes. Development. 2010;137:845–57. doi:10.1242/dev.039651.

12. Loh KM, Amerongen R van, Nusse R. Generating cellular diversity and spatial form: Wnt signaling

and the evolution of multicellular animals. Dev Cell. 2016;38:643–55. doi:10.1016/j.devcel.2016.08.011.

13. Tada M, Smith JC. *Xwnt11* is a target of *Xenopus* Brachyury: Regulation of gastrulation movements via Dishevelled, but not through the canonical Wnt pathway. Development. 2000;127:2227–38. doi:10.1242/dev.127.10.2227.

14. Heisenberg CP, Tada M, Rauch GJ, Saúde L, Concha ML, Geisler R, et al. Silberblick/Wnt11 mediates convergent extension movements during zebrafish gastrulation. Nature. 2000;405:76–81. doi:10.1038/35011068.

15. Yamanaka H, Moriguchi T, Masuyama N, Kusakabe M, Hanafusa H, Takada R, et al. JNK functions in the non-canonical Wnt pathway to regulate convergent extension movements in vertebrates. EMBO Rep. 2002;3:69–75. doi:10.1093/embo-reports/kvf008.

16. Kilian B, Mansukoski H, Barbosa FC, Ulrich F, Tada M, Heisenberg CP. The role of Ppt/Wnt5 in regulating cell shape and movement during zebrafish gastrulation. Mech Dev. 2003;120:467–76. doi:10.1016/s0925-4773(03)00004-2.

17. Ulrich F, Concha ML, Heid PJ, Voss E, Witzel S, Roehl H, et al. Slb/Wnt11 controls hypoblast cell migration and morphogenesis at the onset of zebrafish gastrulation. Development. 2003;130:5375–84. doi:10.1242/dev.00758.

18. Lee J-Y, Marston DJ, Walston T, Hardin J, Halberstadt A, Goldstein B. Wnt/Frizzled signaling controls *C. elegans* gastrulation by activating actomyosin contractility. Curr Biol. 2006;16:1986–97. doi:10.1016/j.cub.2006.08.090.

19. Kumburegama S, Wijesena N, Xu R, Wikramanayake AH. Strabismus-mediated primary archenteron invagination is uncoupled from Wnt/β-catenin-dependent endoderm cell fate specification in *Nematostella vectensis* (Anthozoa, Cnidaria): Implications for the evolution of gastrulation. Evodevo. 2011;2:2. doi:10.1186/2041-9139-2-2.

20. James RG, Conrad WH, Moon RT. β-catenin-independent wnt pathways: Signals, core proteins, and effectors. In: Wnt signaling: Pathway methods and mammalian models. Vincan E, editor. Totowa, NJ: Humana Press; 2008. p. 131–44. doi:10.1007/978-1-59745-249-6_10.

21. Schubert M, Holland LZ, Stokes MD, Holland ND. Three amphioxus *Wnt* genes (*AmphiWnt3*, *AmphiWnt5*, and *AmphiWnt6*) associated with the tail bud: The evolution of somitogenesis in chordates. Dev Biol. 2001;240:262–73. doi:10.1006/dbio.2001.0460.

22. Kusserow A, Pang K, Sturm C, Hrouda M, Lentfer J, Schmidt HA, et al. Unexpected complexity of the Wnt gene family in a sea anemone. Nature. 2005;433:156–60. doi:10.1038/nature03158.

23. Lee PN, Pang K, Matus DQ, Martindale MQ. A WNT of things to come: Evolution of wnt signaling and polarity in cnidarians. Semin Cell Dev Biol. 2006;17:157–67. doi:10.1016/j.semcdb.2006.05.002.

24. Guder C, Philipp I, Lengfeld T, Watanabe H, Hobmayer B, Holstein TW. The Wnt code: Cnidarians

signal the way. Oncogene. 2006;25:7450–60. doi:10.1038/sj.onc.1210052.

25. Janssen R, Le Gouar M, Pechmann M, Poulin F, Bolognesi R, Schwager EE, et al. Conservation, loss, and redeployment of Wnt ligands in protostomes: Implications for understanding the evolution of segment formation. BMC Evol Biol. 2010;10:374. doi:10.1186/1471-2148-10-374.

26. Hunt P, Krumlauf R. Deciphering the hox code: Clues to patterning branchial regions of the head. Cell. 1991;66:1075–8. doi:10.1016/0092-8674(91)90029-X.

27. Amerongen R van, Nusse R. Towards an integrated view of Wnt signaling in development. Development. 2009;136:3205–14. doi:10.1242/dev.033910.

28. Niehrs C. The complex world of WNT receptor signalling. Nat Rev Mol Cell Biol. 2012;13:767–79. doi:10.1038/nrm3470.

29. Umbhauer M, Djiane A, Goisset C, Penzo-Méndez A, Riou JF, Boucaut JC, et al. The C-terminal cytoplasmic Lys-Thr-X-X-X-Trp motif in frizzled receptors mediates Wnt/β-catenin signalling. EMBO J. 2000;19:4944–54. doi:10.1093/emboj/19.18.4944.

30. Mikels AJ, Nusse R. Purified Wnt5a protein activates or inhibits β-catenin-TCF signaling depending on receptor context. PLoS Biol. 2006;4:e115. doi:10.1371/journal.pbio.0040115.

31. Amerongen R van, Mikels A, Nusse R. Alternative wnt signaling is initiated by distinct receptors. Sci Signal. 2008;1:re9. doi:10.1126/scisignal.135re9.

32. Hejnol A, Lowe CJ. Embracing the comparative approach: How robust phylogenies and broader developmental sampling impacts the understanding of nervous system evolution. Philos Trans R Soc Lond B Biol Sci. 2015;370. doi:10.1098/rstb.2015.0045.

33. Akam M. Hox and HOM: Homologous gene clusters in insects and vertebrates. Cell. 1989;57:347–9. http://www.ncbi.nlm.nih.gov/pubmed/2566382.

34. McGinnis W, Krumlauf R. Homeobox genes and axial patterning. Cell. 1992;68:283–302. http://www.ncbi.nlm.nih.gov/pubmed/1346368.

35. Dickinson WJ. Molecules and morphology: Where's the homology? Trends Genet. 1995;11:119–21. http://www.ncbi.nlm.nih.gov/pubmed/7732580.

36. Kelly GM, Greenstein P, Erezyilmaz DF, Moon RT. Zebrafish *wnt8* and *wnt8b* share a common activity but are involved in distinct developmental pathways. Development. 1995;121:1787–99. doi:10.1242/dev.121.6.1787.

37. Hollyday M, McMahon JA, McMahon AP. Wnt expression patterns in chick embryo nervous system. Mech Dev. 1995;52:9–25. doi:10.1016/0925-4773(95)00385-e.

38. Pruitt MM, Letcher EJ, Chou H-C, Bastin BR, Schneider SQ. Expression of the *wnt* gene complement in a spiral-cleaving embryo and trochophore larva. Int J Dev Biol. 2014;58:563–73. doi:10.1387/ijdb.140084ss.

39. Darras S, Fritzenwanker JH, Uhlinger KR, Farrelly E, Pani AM, Hurley IA, et al. Anteroposterior axis patterning by early canonical Wnt signaling during hemichordate development. PLoS Biol. 2018;16:e2003698. doi:10.1371/journal.pbio.2003698.

40. Wiese KE, Nusse R, Amerongen R van. Wnt signalling: Conquering complexity. Development. 2018;145:dev165902. doi:10.1242/dev.165902.

41. Hejnol A. A twist in time—the evolution of spiral cleavage in the light of animal phylogeny. Integr Comp Biol. 2010;50:695–706. doi:10.1093/icb/icq103.

42. Martín-Durán JM, Marlétaz F. Unravelling spiral cleavage. Development. 2020;147. doi:10.1242/dev.181081.

43. Murat S, Hopfen C, McGregor AP. The function and evolution of Wnt genes in arthropods. Arthropod Struct Dev. 2010;39:446–52. doi:10.1016/j.asd.2010.05.007.

44. Holstein TW. The evolution of the Wnt pathway. Cold Spring Harb Perspect Biol. 2012;4:a007922. doi:10.1101/cshperspect.a007922.

45. Chavarria RA, Game M, Arbelaez B, Ramnarine C, Snow ZK, Smith FW. Extensive loss of Wnt genes in Tardigrada. BMC Ecol Evol. 2021;21:223. doi:10.1186/s12862-021-01954-y.

46. Prud'homme B, Lartillot N, Balavoine G, Adoutte A, Vervoort M. Phylogenetic analysis of the Wnt gene family. Insights from lophotrochozoan members. Curr Biol. 2002;12:1395. doi:10.1016/s0960-9822(02)01068-0.

47. Cho S-J, Vallès Y, Giani VC Jr, Seaver EC, Weisblat DA. Evolutionary dynamics of the *wnt* gene family: A lophotrochozoan perspective. Mol Biol Evol. 2010;27:1645–58. doi:10.1093/molbev/msq052.

48. Hyman LH. The lophophorate coelomates—Phylum Brachiopoda. In: Smaller coelomate groups. Boell EJ, editor. New York: McGraw-Hill Book Company, Inc; 1959. p. 516–609.

49. Conklin EG. The embryology of a brachiopod, *Terebratulina septentrionalis* Couthouy. Proc Am Philos Soc. 1902;41:41–76. doi:10.2307/983525.

50. Franzén Å. On larval development and metamorphosis in *Terebratulina*, Brachiopoda. Zoologiska Bidrag Fran Uppsala. 1969;38:155–74.

51. Flammer LI. Embryology of the brachiopod *Terebratalia transversa*. Master's thesis. University of Washington; 1963.

52. Stricker SA, Reed CG. The ontogeny of shell secretion in *Terebratalia transversa* (Brachiopoda, Articulata). I. Development of the mantle. J Morphol. 1985;183:233–50. doi:10.1002/jmor.1051830302.

53. Stricker SA, Reed CG. Development of the pedicle in the articulate brachiopod *Terebratalia transversa* (Brachiopoda, Terebratulida). Zoomorphology. 1985;105:253–64. doi:10.1007/BF00311968.

54. Freeman G. Metamorphosis in the brachiopod *Terebratalia*: Evidence for a role of calcium channel function and the dissociation of shell formation from settlement. Biol Bull. 1993;184:15–24.

doi:10.2307/1542376.

55. Freeman G. Regional specification during embryogenesis in the articulate brachiopod *Terebratalia*. Dev Biol. 1993;160:196–213. doi:10.1006/dbio.1993.1298.

56. Martín-Durán JM, Passamaneck YJ, Martindale MQ, Hejnol A. The developmental basis for the recurrent evolution of deuterostomy and protostomy. Nat Ecol Evol. 2016;1:5. doi:10.1038/s41559-016-0005.

57. Vellutini BC, Hejnol A. Expression of segment polarity genes in brachiopods supports a non-segmental ancestral role of *engrailed* for bilaterians. Sci Rep. 2016;6:32387. doi:10.1038/srep32387.

58. Nusse R, Varmus HE. Wnt genes. Cell. 1992;69:1073–87. doi:10.1016/0092-8674(92)90630-U.

59. Croce JC, McClay DR. Evolution of the Wnt Pathways. In: Wnt signaling. Vincan E, editor. Totowa, NJ: Humana Press; 2009. p. 3–18. doi:10.1007/978-1-60327-469-2_1.

60. Huang H-C, Klein PS. The Frizzled family: Receptors for multiple signal transduction pathways. Genome Biol. 2004;5:234. doi:10.1186/gb-2004-5-7-234.

61. MacDonald BT, He X. Frizzled and LRP5/6 receptors for Wnt/β-catenin signaling. Cold Spring Harb Perspect Biol. 2012;4. doi:10.1101/cshperspect.a007880.

62. Croce JC, Wu S-Y, Byrum C, Xu R, Duloquin L, Wikramanayake AH, et al. A genome-wide survey of the evolutionarily conserved Wnt pathways in the sea urchin *Strongylocentrotus purpuratus*. Dev Biol. 2006;300:121–31. doi:10.1016/j.ydbio.2006.08.045.

63. Kawano Y, Kypta R. Secreted antagonists of the Wnt signalling pathway. J Cell Sci. 2003;116:2627–34. doi:10.1242/jcs.00623.

64. Bovolenta P, Esteve P, Ruiz JM, Cisneros E, Lopez-Rios J. Beyond Wnt inhibition: New functions of secreted Frizzled-related proteins in development and disease. J Cell Sci. 2008;121:737–46. doi:10.1242/jcs.026096.

65. Niehrs C. Function and biological roles of the Dickkopf family of Wnt modulators. Oncogene. 2006;25:7469–81. doi:10.1038/sj.onc.1210054.

66. Cruciat C-M, Niehrs C. Secreted and transmembrane Wnt inhibitors and activators. Cold Spring Harb Perspect Biol. 2013;5:a015081. doi:10.1101/cshperspect.a015081.

67. Hsieh JC, Kodjabachian L, Rebbert ML, Rattner A, Smallwood PM, Samos CH, et al. A new secreted protein that binds to Wnt proteins and inhibits their activities. Nature. 1999;398:431–6. doi:10.1038/18899.

68. Simons M, Mlodzik M. Planar cell polarity signaling: From fly development to human disease. Annu Rev Genet. 2008;42:517–40. doi:10.1146/annurev.genet.42.110807.091432.

69. Gao B. Wnt regulation of planar cell polarity (PCP). Curr Top Dev Biol. 2012;101:263–95. doi:10.1016/B978-0-12-394592-1.00008-9.

70. Wallingford JB, Habas R. The developmental biology of Dishevelled: An enigmatic protein governing cell fate and cell polarity. Development. 2005;132:4421–36. doi:10.1242/dev.02068.

71. Gao C, Chen Y-G. Dishevelled: The hub of Wnt signaling. Cell Signal. 2010;22:717–27. doi:10.1016/j.cellsig.2009.11.021.

72. Feiguin F, Hannus M, Mlodzik M, Eaton S. The ankyrin repeat protein Diego mediates Frizzled-dependent planar polarization. Dev Cell. 2001;1:93–101. doi:10.1016/s1534-5807(01)00010-7.

73. Schwarz-Romond T, Asbrand C, Bakkers J, Kühl M, Schaeffer H-J, Huelsken J, et al. The ankyrin repeat protein Diversin recruits Casein kinase iepsilon to the beta-catenin degradation complex and acts in both canonical Wnt and Wnt/JNK signaling. Genes Dev. 2002;16:2073–84. doi:10.1101/gad.230402.

74. Gubb D, Green C, Huen D, Coulson D, Johnson G, Tree D, et al. The balance between isoforms of the prickle LIM domain protein is critical for planar polarity in *Drosophila* imaginal discs. Genes Dev. 1999;13:2315–27. doi:10.1101/gad.13.17.2315.

75. Jenny A, Reynolds-Kenneally J, Das G, Burnett M, Mlodzik M. Diego and Prickle regulate Frizzled planar cell polarity signalling by competing for Dishevelled binding. Nat Cell Biol. 2005;7:691–7. doi:10.1038/ncb1271.

76. Usui T, Shima Y, Shimada Y, Hirano S, Burgess RW, Schwarz TL, et al. Flamingo, a seven-pass transmembrane cadherin, regulates planar cell polarity under the control of Frizzled. Cell. 1999;98:585–95. doi:10.1016/s0092-8674(00)80046-x.

77. Chae J, Kim MJ, Goo JH, Collier S, Gubb D, Charlton J, et al. The *Drosophila* tissue polarity gene *starry night* encodes a member of the protocadherin family. Development. 1999;126:5421–9. doi:10.1242/dev.126.23.5421.

78. Katoh K, Standley DM. MAFFT multiple sequence alignment software version 7: Improvements in performance and usability. Mol Biol Evol. 2013;30:772–80. doi:10.1093/molbev/mst010.

79. Butler MT, Wallingford JB. Planar cell polarity in development and disease. Nat Rev Mol Cell Biol. 2017;18:375–88. doi:10.1038/nrm.2017.11.

80. Noselli S, Agnès F. Roles of the JNK signaling pathway in *Drosophila* morphogenesis. Curr Opin Genet Dev. 1999;9:466–72. doi:10.1016/S0959-437X(99)80071-9.

81. Santagata S. Evaluating neurophylogenetic patterns in the larval nervous systems of brachiopods and their evolutionary significance to other bilaterian phyla. J Morphol. 2011;272:1153–69. doi:10.1002/jmor.10975.

82. Range RC, Angerer RC, Angerer LM. Integration of canonical and noncanonical Wnt signaling pathways patterns the neuroectoderm along the anterior-posterior axis of sea urchin embryos. PLoS Biol. 2013;11:e1001467. doi:10.1371/journal.pbio.1001467.

83. Khadka A, Martínez-Bartolomé M, Burr SD, Range RC. A novel gene's role in an ancient mech-

anism: Secreted Frizzled-related protein 1 is a critical component in the anterior-posterior Wnt signaling network that governs the establishment of the anterior neuroectoderm in sea urchin embryos. Evodevo. 2018;9:1. doi:10.1186/s13227-017-0089-3.

84. Lagutin OV, Zhu CC, Kobayashi D, Topczewski J, Shimamura K, Puelles L, et al. Six3 repression of Wnt signaling in the anterior neuroectoderm is essential for vertebrate forebrain development. Genes Dev. 2003;17:368–79. doi:10.1101/gad.1059403.

85. Wei Z, Yaguchi J, Yaguchi S, Angerer RC, Angerer LM. The sea urchin animal pole domain is a Six3-dependent neurogenic patterning center. Development. 2009;136:1179–89. doi:10.1242/dev.032300.

86. Posnien N, Koniszewski NDB, Hein HJ, Bucher G. Candidate gene screen in the red flour beetle *Tribolium* reveals *six3* as ancient regulator of anterior median head and central complex development. PLoS Genet. 2011;7:e1002416. doi:10.1371/journal.pgen.1002416.

87. Sinigaglia C, Busengdal H, Leclère L, Technau U, Rentzsch F. The bilaterian head patterning gene *six3/6* controls aboral domain development in a cnidarian. PLoS Biol. 2013;11:e1001488. doi:10.1371/journal.pbio.1001488.

88. Erter CE, Wilm TP, Basler N, Wright CV, Solnica-Krezel L. Wnt8 is required in lateral mesendodermal precursors for neural posteriorization in vivo. Development. 2001;128:3571–83. doi:10.1242/dev.128.18.3571.

89. Lekven AC, Thorpe CJ, Waxman JS, Moon RT. Zebrafish *wnt8* encodes two wnt8 proteins on a bicistronic transcript and is required for mesoderm and neurectoderm patterning. Dev Cell. 2001;1:103–14. doi:10.1016/s1534-5807(01)00007-7.

90. Kim S-H, Shin J, Park H-C, Yeo S-Y, Hong S-K, Han S, et al. Specification of an anterior neuroectoderm patterning by Frizzled8a-mediated Wnt8b signalling during late gastrulation in zebrafish. Development. 2002;129:4443–55. doi:10.1242/dev.129.19.4443.

91. Rhinn M, Lun K, Luz M, Werner M, Brand M. Positioning of the midbrain-hindbrain boundary organizer through global posteriorization of the neuroectoderm mediated by Wnt8 signaling. Development. 2005;132:1261–72. doi:10.1242/dev.01685.

92. Leclère L, Bause M, Sinigaglia C, Steger J, Rentzsch F. Development of the aboral domain in *Nematostella* requires *β-catenin* and the opposing activities of *Six3/6* and *Frizzled5/8*. Development. 2016;143:1766–77. doi:10.1242/dev.120931.

93. Santagata S, Resh C, Hejnol A, Martindale MQ, Passamaneck YJ. Development of the larval anterior neurogenic domains of *Terebratalia transversa* (Brachiopoda) provides insights into the diversification of larval apical organs and the spiralian nervous system. Evodevo. 2012;3:3. doi:10.1186/2041-9139-3-3.

94. Parr BA, Shea MJ, Vassileva G, McMahon AP. Mouse Wnt genes exhibit discrete domains

of expression in the early embryonic CNS and limb buds. Development. 1993;119:247–61. doi:10.1242/dev.119.1.247.

95. Rhinn M, Brand M. The midbrain–hindbrain boundary organizer. Curr Opin Neurobiol. 2001;11:34–42. doi:10.1016/S0959-4388(00)00171-9.

96. Winn RA, Marek L, Han S-Y, Rodriguez K, Rodriguez N, Hammond M, et al. Restoration of Wnt-7a expression reverses non-small cell lung cancer cellular transformation through Frizzled-9-mediated growth inhibition and promotion of cell differentiation. J Biol Chem. 2005;280:19625–34. doi:10.1074/jbc.M409392200.

97. Freeman G, Lundelius J. The transition from planktotrophy to lecithotrophy in larvae of Lower Palaeozoic Rhynchonelliform brachiopods. Lethaia. 2005;38:219–54. doi:10.1080/00241160510013330.

98. Qian D, Jones C, Rzadzinska A, Mark S, Zhang X, Steel KP, et al. Wnt5a functions in planar cell polarity regulation in mice. Dev Biol. 2007;306:121–33. doi:10.1016/j.ydbio.2007.03.011.

99. Yamaguchi TP, Bradley A, McMahon AP, Jones S. A *Wnt5a* pathway underlies outgrowth of multiple structures in the vertebrate embryo. Development. 1999;126:1211–23. doi:10.1242/dev.126.6.1211.

100. Hogvall M, Schönauer A, Budd GE, McGregor AP, Posnien N, Janssen R. Analysis of the *Wnt* gene repertoire in an onychophoran provides new insights into the evolution of segmentation. Evodevo. 2014;5:14. doi:10.1186/2041-9139-5-14.

101. Jho E-H, Zhang T, Domon C, Joo C-K, Freund J-N, Costantini F. Wnt/β-catenin/Tcf signaling induces the transcription of Axin2, a negative regulator of the signaling pathway. Mol Cell Biol. 2002;22:1172–83. doi:10.1128/MCB.22.4.1172-1183.2002.

102. Schultz DT, Haddock SHD, Bredeson JV, Green RE, Simakov O, Rokhsar DS. Ancient gene linkages support ctenophores as sister to other animals. Nature. 2023;1–8. doi:10.1038/s41586-023-05936-6.

103. Pang K, Ryan JF, NISC Comparative Sequencing Program, Mullikin JC, Baxevanis AD, Martindale MQ. Genomic insights into Wnt signaling in an early diverging metazoan, the ctenophore *Mnemiopsis leidyi*. Evodevo. 2010;1:10. doi:10.1186/2041-9139-1-10.

104. Bastin BR, Chou H-C, Pruitt MM, Schneider SQ. Structure, phylogeny, and expression of the frizzled-related gene family in the lophotrochozoan annelid *Platynereis dumerilii*. Evodevo. 2015;6:37. doi:10.1186/s13227-015-0032-4.

105. Niedermoser I, Lebedeva T, Genikhovich G. Sea anemone Frizzled receptors play partially redundant roles in oral-aboral axis patterning. Development. 2022;149:dev200785. doi:10.1242/dev.200785.

106. Robert N, Lhomond G, Schubert M, Croce JC. A comprehensive survey of *wnt* and *frizzled* expression in the sea urchin *Paracentrotus lividus*. Genesis. 2014;52:235–50. doi:10.1002/dvg.22754.

107. McCauley BS, Akyar E, Filliger L, Hinman VF. Expression of *wnt* and *frizzled* genes during early sea star development. Gene Expr Patterns. 2013;13:437–44. doi:10.1016/j.gep.2013.07.007.

108. Qian G, Li G, Chen X, Wang Y. Characterization and embryonic expression of four amphioxus *Frizzled* genes with important functions during early embryogenesis. Gene Expr Patterns. 2013;13:445–53. doi:10.1016/j.gep.2013.08.003.

109. Somorjai IML, Martí-Solans J, Diaz-Gracia M, Nishida H, Imai KS, Escrivà H, et al. Wnt evolution and function shuffling in liberal and conservative chordate genomes. Genome Biol. 2018;19:98. doi:10.1186/s13059-018-1468-3.

110. Reed CG. Phylum Brachiopoda. In: Reproduction and development of marine invertebrates of the northern pacific coast. Strathmann MF, editor. University of Washington Press; 1987. p. 486–93.

111. Bray NL, Pimentel H, Melsted P, Pachter L. Near-optimal probabilistic RNA-seq quantification. Nat Biotechnol. 2016;34:525–7. doi:10.1038/nbt.3519.

112. Love MI, Huber W, Anders S. Moderated estimation of fold change and dispersion for RNA-seq data with DESeq2. Genome Biol. 2014;15:550. doi:10.1186/s13059-014-0550-8.

113. Kolde R. Pheatmap: Pretty heatmaps. computer software. Github. https://github.com/raivokolde/pheatmap. Accessed 29 Dec 2021.

114. Wickham H. ggplot2: Elegant graphics for data analysis. Springer-Verlag New York; 2016. https://ggplot2.tidyverse.org.

115. R Core Team. R: A language and environment for statistical computing. computer software. R Foundation for Statistical Computing; 1993. http://www.r-project.org. Accessed 2023.

116. RStudio Team. RStudio: Integrated development environment for r. computer software. Boston, MA: RStudio, PBC.; 2011. http://www.rstudio.com/. Accessed 2023.

117. Camacho C, Coulouris G, Avagyan V, Ma N, Papadopoulos J, Bealer K, et al. BLAST+: Architecture and applications. BMC Bioinformatics. 2009;10:421. doi:10.1186/1471-2105-10-421.

118. Talavera G, Castresana J. Improvement of phylogenies after removing divergent and ambiguously aligned blocks from protein sequence alignments. Syst Biol. 2007;56:564–77. doi:10.1080/10635150701472164.

119. Okonechnikov K, Golosova O, Fursov M, UGENE team. Unipro UGENE: A unified bioinformatics toolkit. Bioinformatics. 2012;28:1166–7. doi:10.1093/bioinformatics/bts091.

120. Stamatakis A. RAxML version 8: A tool for phylogenetic analysis and post-analysis of large phylogenies. Bioinformatics. 2014;30:1312–3. doi:10.1093/bioinformatics/btu033.

121. Letunic I, Bork P. Interactive tree of life (iTOL) v3: An online tool for the display and annotation of phylogenetic and other trees. Nucleic Acids Res. 2016;44:W242–5. doi:10.1093/nar/gkw290.

122. Untergasser A, Cutcutache I, Koressaar T, Ye J, Faircloth BC, Remm M, et al. Primer3—new capabilities and interfaces. Nucleic Acids Res. 2012;40:e115. doi:10.1093/nar/gks596.

123. Hejnol A. *In situ* protocol for embryos and juveniles of *Convolutriloba longifissura*. Protoc Exch.

2008. doi:10.1038/nprot.2008.201.

124. Schindelin J, Arganda-Carreras I, Frise E, Kaynig V, Longair M, Pietzsch T, et al. Fiji: An open-source platform for biological-image analysis. Nat Methods. 2012;9:676–82. doi:10.1038/nmeth.2019.

125. Holland LZ, Holland NN, Schubert M. Developmental expression of *AmphiWnt1*, an amphioxus gene in the *Wnt1/wingless* subfamily. Dev Genes Evol. 2000;210:522–4. doi:10.1007/s004270050342.

126. Schubert M, Holland LZ, Holland ND. Characterization of two amphioxus Wnt genes (AmphiWnt4 and AmphiWnt7b) with early expression in the developing central nervous system. Dev Dyn. 2000;217:205–15. doi:10.1002/(SICI)1097-0177(200002)217:2<205::AID-DVDY7>3.0.CO;2-F.

127. Schubert M, Holland LZ, Panopoulou GD, Lehrach H, Holland ND. Characterization of amphioxus AmphiWnt8: Insights into the evolution of patterning of the embryonic dorsoventral axis. Evol Dev. 2000;2:85–92. https://www.ncbi.nlm.nih.gov/pubmed/11258394.

128. Schubert M, Holland LZ, Holland ND. Characterization of an amphioxus wnt gene, AmphiWnt11, with possible roles in myogenesis and tail outgrowth. Genesis. 2000;27:1–5. doi:10.1002/1526-968x(200005)27:1<1::aid-gene10>3.3.co;2-v.

129. Yu J-K, Satou Y, Holland ND, Shin-I T, Kohara Y, Satoh N, et al. Axial patterning in cephalochordates and the evolution of the organizer. Nature. 2007;445:613–7. doi:10.1038/nature05472.

130. Onai T, Takai A, Setiamarga DHE, Holland LZ. Essential role of Dkk3 for head formation by inhibiting Wnt/β-catenin and Nodal/Vg1 signaling pathways in the basal chordate amphioxus. Evol Dev. 2012;14:338–50. doi:10.1111/j.1525-142X.2012.00552.x.

131. Croce J, Duloquin L, Lhomond G, McClay DR, Gache C. Frizzled5/8 is required in secondary mesenchyme cells to initiate archenteron invagination during sea urchin development. Development. 2006;133:547–57. doi:10.1242/dev.02218.

132. Lhomond G, McClay DR, Gache C, Croce JC. Frizzled1/2/7 signaling directs β-catenin nuclearisation and initiates endoderm specification in macromeres during sea urchin embryogenesis. Development. 2012;139:816–25. doi:10.1242/dev.072215.

133. Cui M, Siriwon N, Li E, Davidson EH, Peter IS. Specific functions of the wnt signaling system in gene regulatory networks throughout the early sea urchin embryo. Proc Natl Acad Sci U S A. 2014;111:E5029–38. doi:10.1073/pnas.1419141111.

134. Range RC, Wei Z. An anterior signaling center patterns and sizes the anterior neuroectoderm of the sea urchin embryo. Development. 2016;143:1523–33. doi:10.1242/dev.128165.

135. Range RC. Canonical and non-canonical Wnt signaling pathways define the expression domains of Frizzled 5/8 and Frizzled 1/2/7 along the early anterior-posterior axis in sea urchin embryos. Dev Biol. 2018. doi:10.1016/j.ydbio.2018.10.003.

136. Luo Y-J, Takeuchi T, Koyanagi R, Yamada L, Kanda M, Khalturina M, et al. The *Lingula* genome

provides insights into brachiopod evolution and the origin of phosphate biomineralization. Nat Commun. 2015;6:8301. doi:10.1038/ncomms9301.

137. Luo Y-J, Kanda M, Koyanagi R, Hisata K, Akiyama T, Sakamoto H, et al. Nemertean and phoronid genomes reveal lophotrochozoan evolution and the origin of bilaterian heads. Nat Ecol Evol. 2018;2:141–51. doi:10.1038/s41559-017-0389-y.

138. Hogvall M, Vellutini BC, Martín-Durán JM, Hejnol A, Budd GE, Janssen R. Embryonic expression of priapulid Wnt genes. Dev Genes Evol. 2019;229:125–35. doi:10.1007/s00427-019-00636-6.

139. Croce J, Range R, Wu S-Y, Miranda E, Lhomond G, Peng JC-F, et al. Wnt6 activates endoderm in the sea urchin gene regulatory network. Development. 2011;138:3297–306. doi:10.1242/dev.058792.

140. Tao Q, Yokota C, Puck H, Kofron M, Birsoy B, Yan D, et al. Maternal Wnt11 activates the canonical wnt signaling pathway required for axis formation in *Xenopus* embryos. Cell. 2005;120:857–71. doi:10.1016/j.cell.2005.01.013.

141. Nasevicius A, Hyatt T, Kim H, Guttman J, Walsh E, Sumanas S, et al. Evidence for a frizzled-mediated wnt pathway required for zebrafish dorsal mesoderm formation. Development. 1998;125:4283–92. doi:10.1242/dev.125.21.4283.

142. Momose T, Derelle R, Houliston E. A maternally localised Wnt ligand required for axial patterning in the cnidarian *Clytia hemisphaerica*. Development. 2008;135:2105–13. doi:10.1242/dev.021543.

Figures

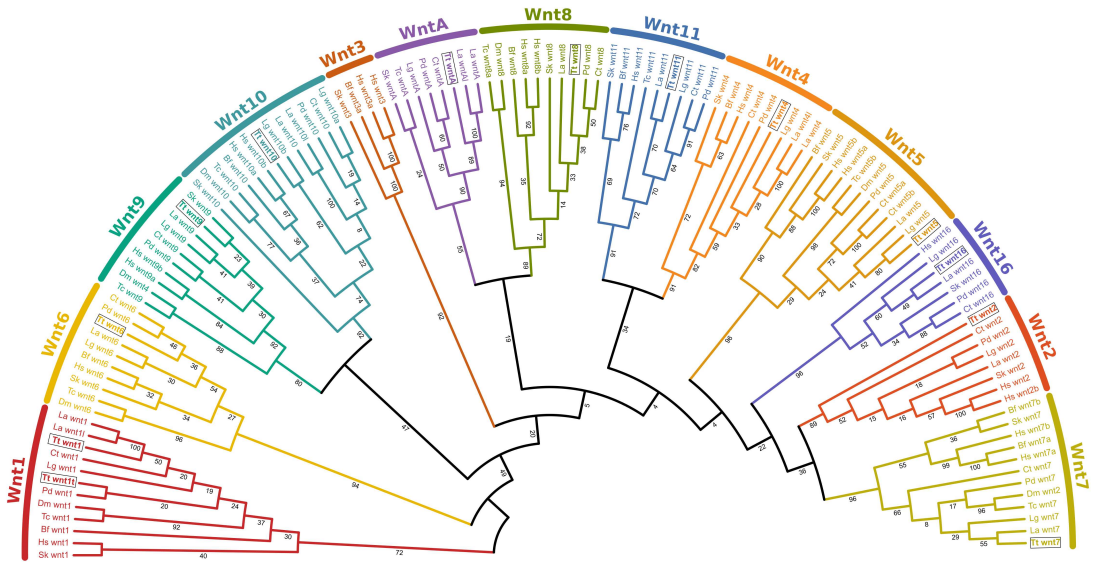

Figure 1: Orthology assignment of *Terebratalia transversa* Wnt genes. Best-scoring tree of a maximum likelihood phylogenetic analysis using the amino acid sequences of known metazoan Wnt genes. The color-coding represents different Wnt subfamilies and the numbers show the support values of individual branches. *Terebratalia transversa* (Tt) orthologs are outlined by a box. The other species are *Branchiostoma floridae* (Bf), *Capitella teleta* (Ct), *Drosophila melanogaster* (Dm), *Homo sapiens* (Hs), *Lingula anatina* (La), *Lottia gigantea* (Lg), *Platynereis dumerilii* (Pd), *Saccoglossus kowalevskii* (Sk), and *Tribolium castaneum* (Tc).

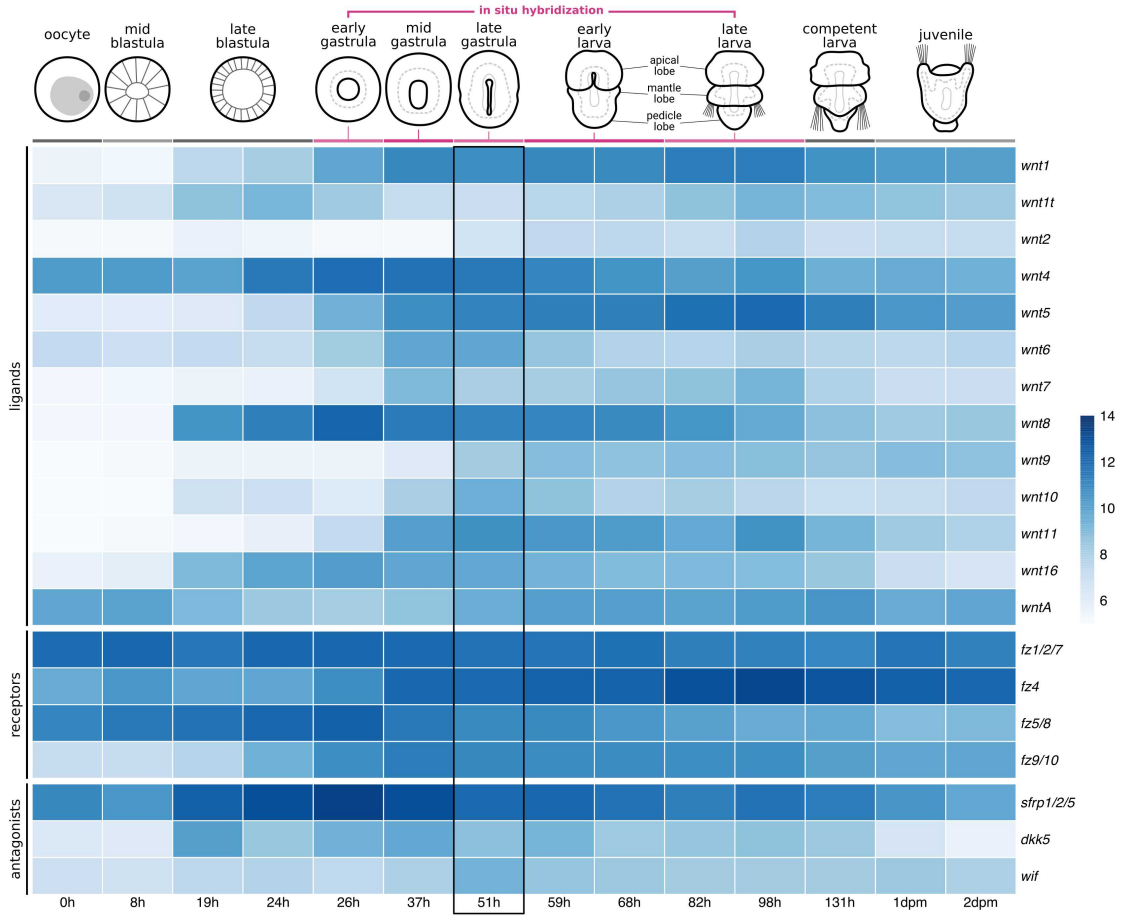

Figure 2: Expression of Wnt signaling components during *Terebratalia transversa* development. The heatmap represents the log-normalized transcript counts for ligands, receptors, and antagonists calculated from stage-specific RNA-seq data. Each cell shows the average value between two replicates. The illustrations depict *T. transversa* developmental stages from the oocyte until the post-metamorphic juvenile. At the late gastrula stage (51h, black outline) all Wnt genes are expressed. The stages we analyzed using *in situ* hybridization (early gastrula to late larva) are highlighted in magenta.

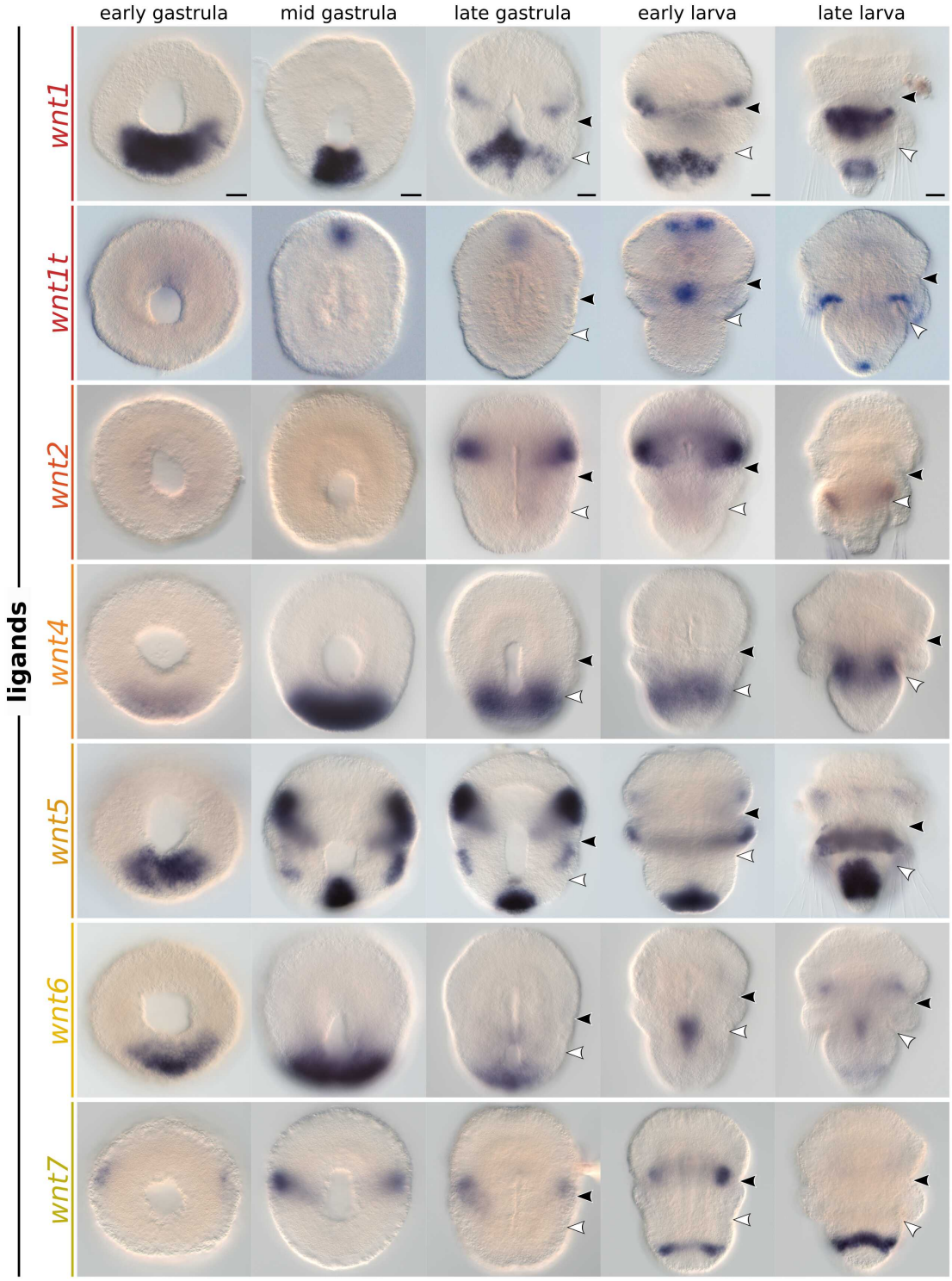

Figure 3: Whole-mount colorimetric *in situ* hybridization of *Terebratalia transversa wnt1*, *wnt1t*, *wnt2*, *wnt4*, *wnt5*, *wnt6*, and *wnt7*. Developmental stages between early gastrula and late larva. The samples are oriented with a blastoporal/ventral view and the anterior end to the top. Black arrowheads indicate the apical–mantle boundary. White arrowheads indicate the mantle–pedicle boundary. Panels for *wnt1* originally published under a Creative Commons Attribution License in [57] and reprinted here for completion. Scale bars = 20µm.

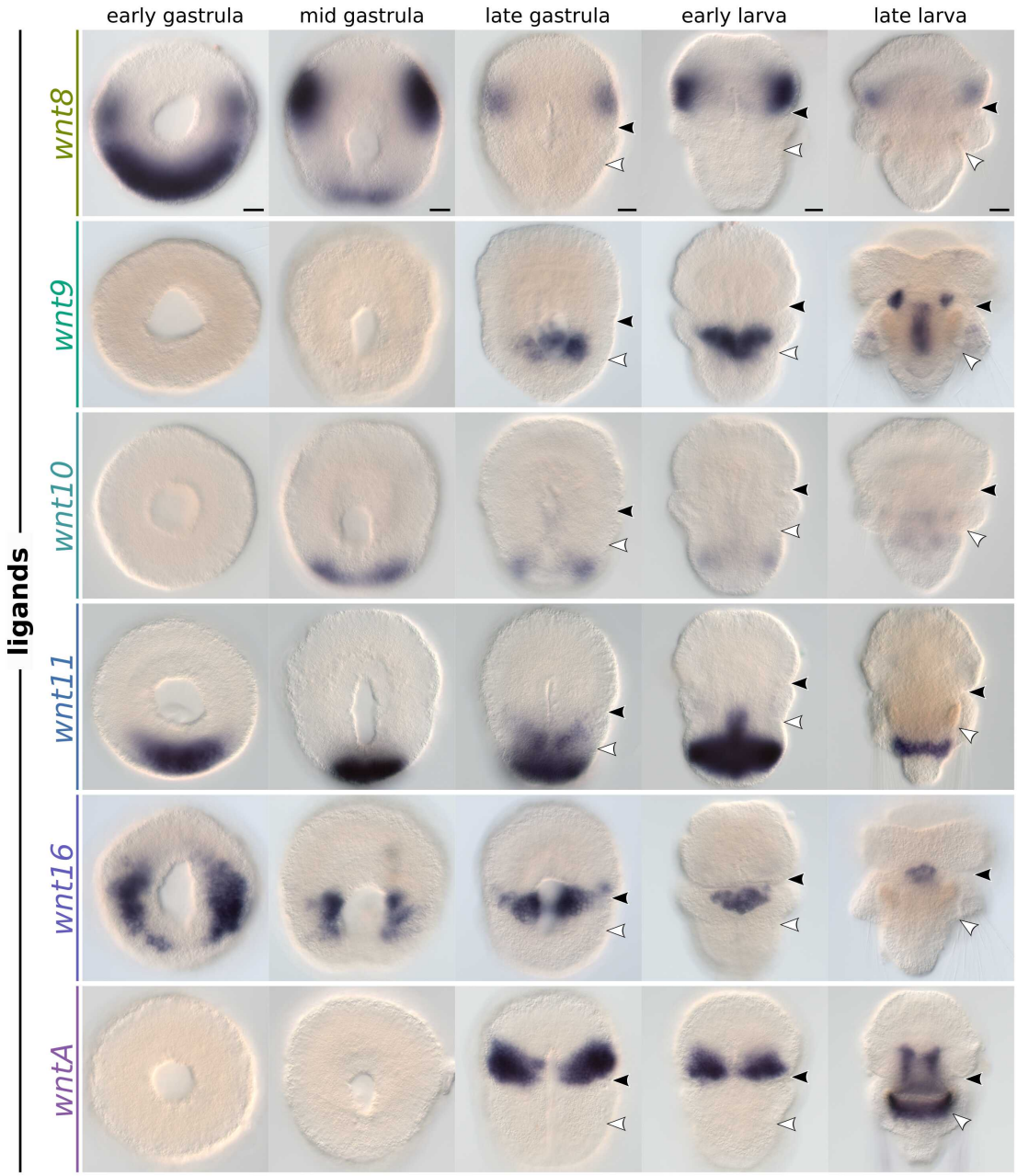

Figure 4: Whole-mount colorimetric *in situ* hybridization of *Terebratalia transversa wnt8*, *wnt9*, *wnt10*, *wnt11*, *wnt16*, and *wntA*. Developmental stages between early gastrula and late larva. The samples are oriented with a blastoporal/ventral view and the anterior end to the top. Black arrowheads indicate the apical–mantle boundary. White arrowheads demarcate the mantle–pedicle boundary. Scale bars = 20µm.

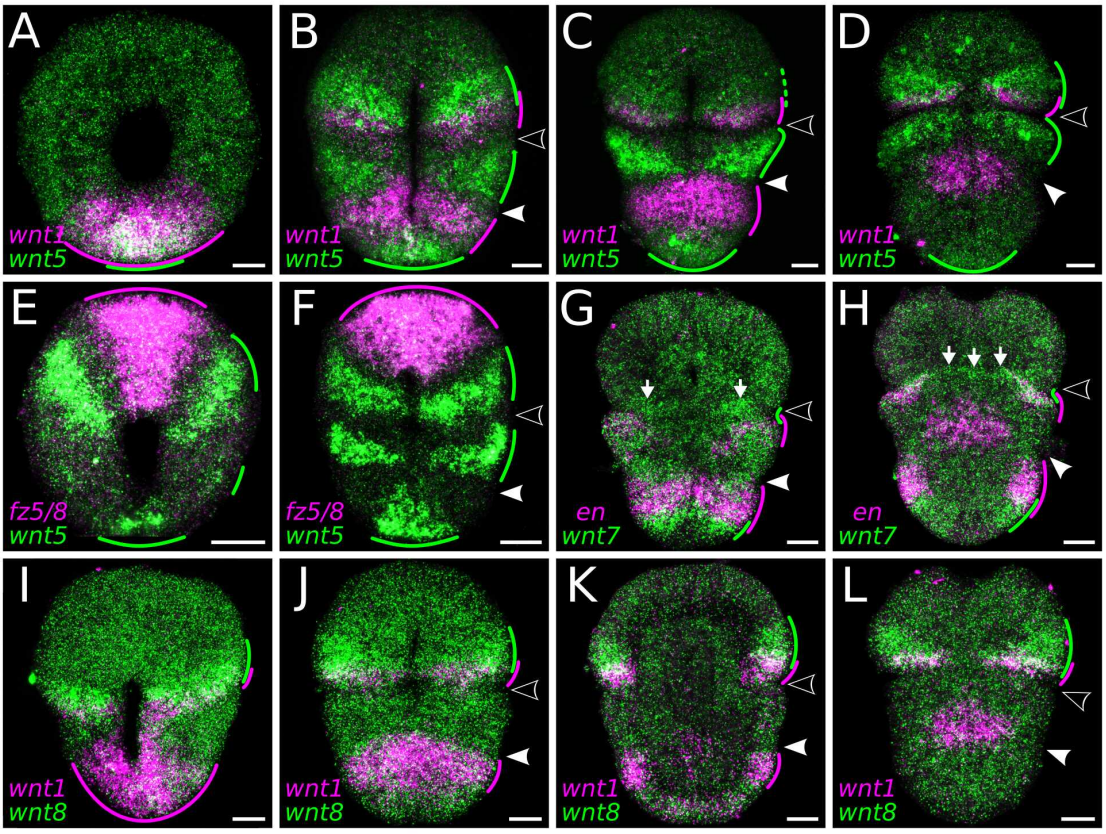

Figure 5: Whole-mount double-fluorescent *in situ* hybridization of *Terebratalia transversa* Wnt genes. (A–D) Expression of *wnt1* (magenta) and *wnt5* (green) in the early gastrula (A), late gastrula (B) and early larva in ventral (C) and dorsal (D) views. (E–F) Expression of *wnt5* (green) and *fz5/8* (magenta) in the mid gastrula (E) and late gastrula (F) in ventral views. (G–H) Expression of *wnt7* (green) *engrailed* (*en*) (magenta) in the early larva in ventral (G) and dorsal (H) views. (I–L) Expression of *wnt1* (magenta) and *wnt8* (green) in the mid gastrula (I) and late gastrula (J) in ventral views, late gastrula in an midbody optical section (K), and early larva in dorsal view (L). Green and magenta lines highlight the extension and overlap between domains. Areas in the tissue where the expression overlaps appear in white. Samples oriented with the anterior end to the top. Black arrowheads indicate the apical–mantle boundary. White arrowheads demarcate the mantle–pedicle boundary. Scale bars = 20μm.

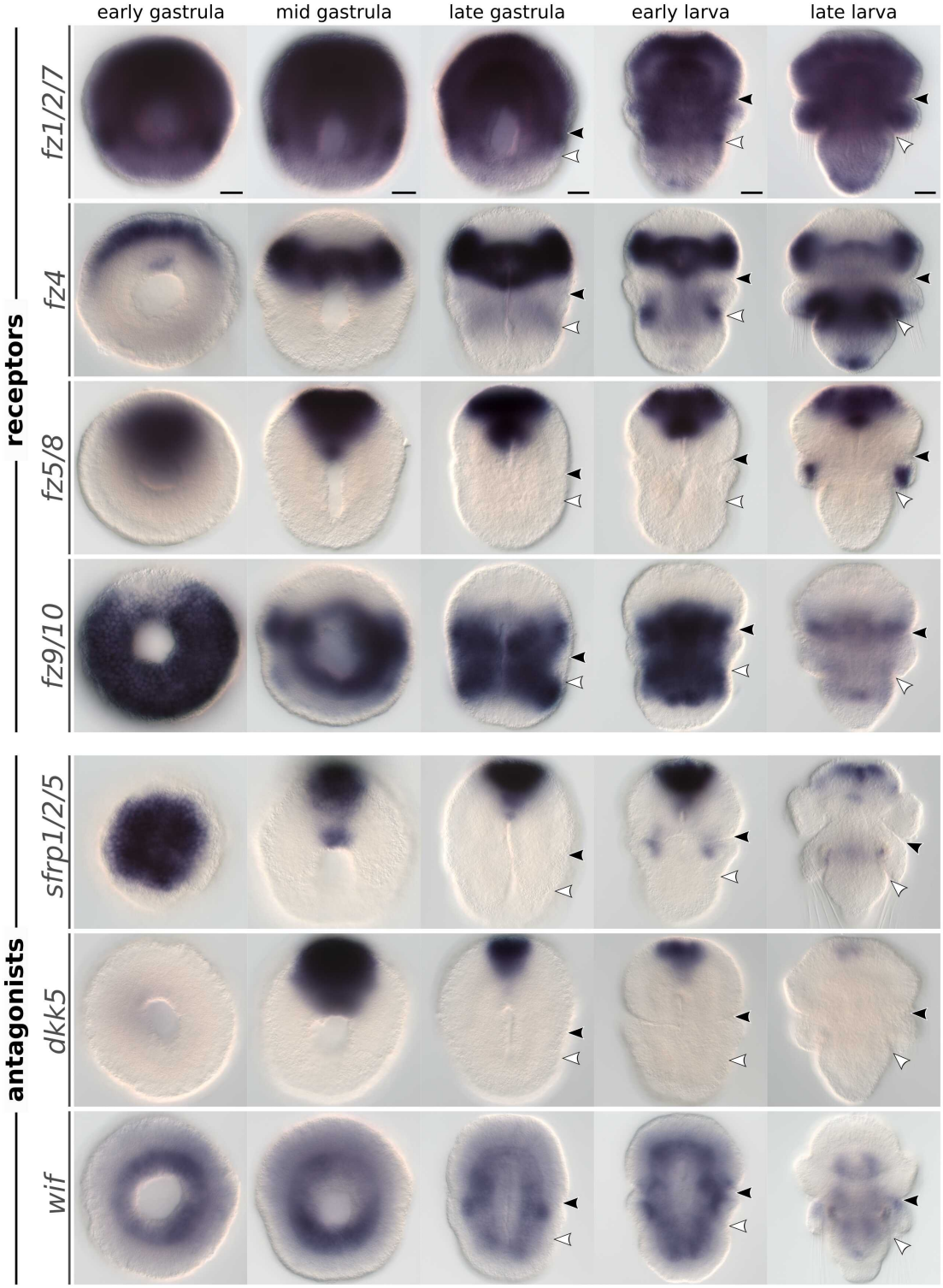

Figure 6: Whole-mount colorimetric *in situ* hybridization of *Terebratalia transversa* Frizzled and Wnt antagonist genes. Developmental stages between early gastrula and late larva for *fz1/2/7*, *fz4*, *fz5/8*, *fz9/10*, *sfrp1/2/5*, *dkk5*, and *wif*. The samples are oriented with a blastoporal/ventral view and the anterior end to the top, except for *sfrp1/2/5* early gastrula showing the apical pole. Black arrowheads indicate the apical–mantle boundary. White arrowheads demarcate the mantle–pedicle boundary. Scale bars = 20µm.

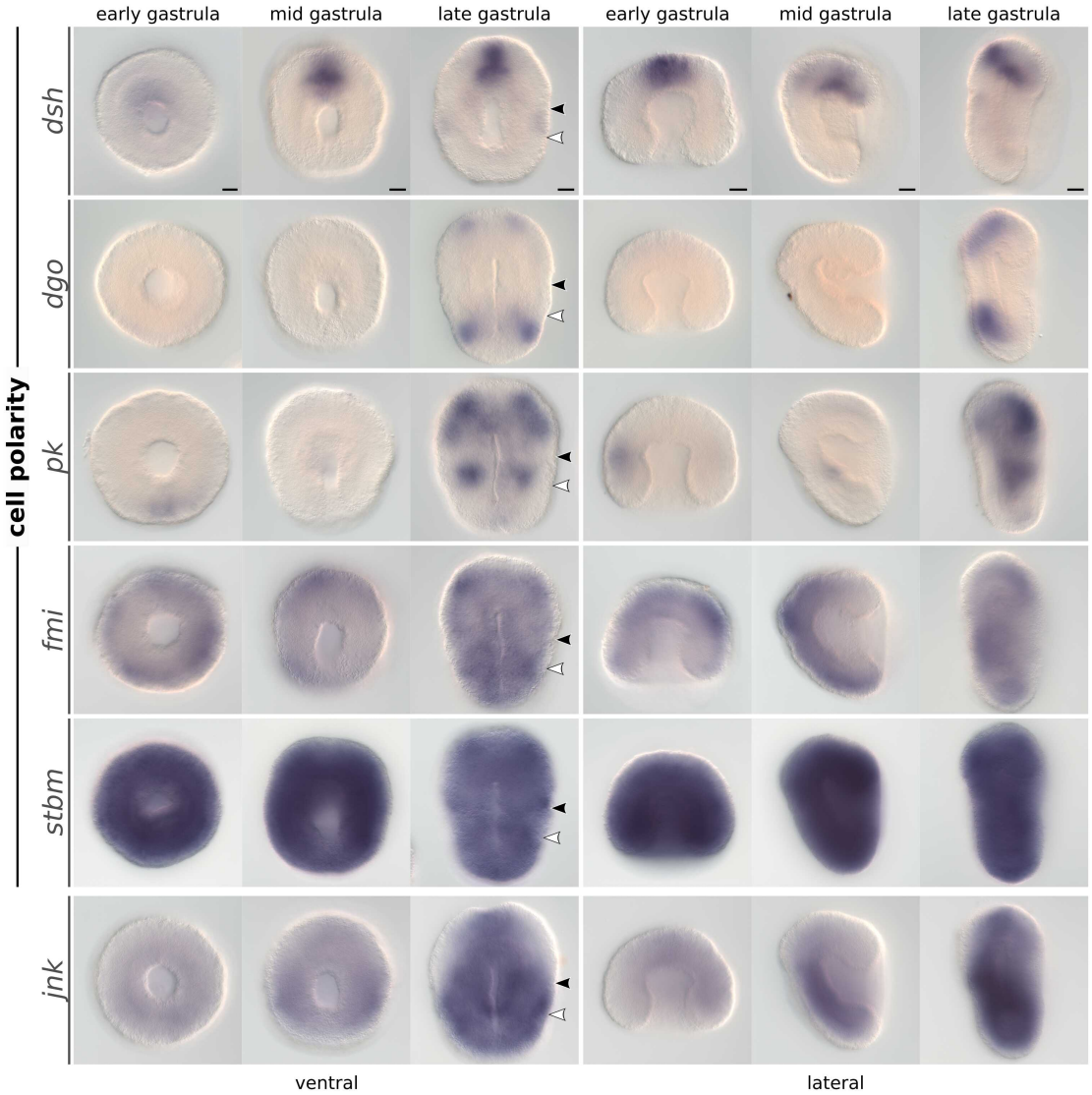

Figure 7: Whole-mount colorimetric *in situ* hybridization of *Terebratalia transversa* Wnt/PCP pathway components. Developmental stages between early gastrula and late gastrula for *dsh*, *dgo*, *pk*, *fmi*, *stbm*, and *jnk*. The samples are oriented in a blastoporal/ventral view (left) and in a lateral view (right). Black arrowheads indicate the apical–mantle boundary. White arrowheads demarcate the mantle–pedicle boundary. Scale bars = 20µm.

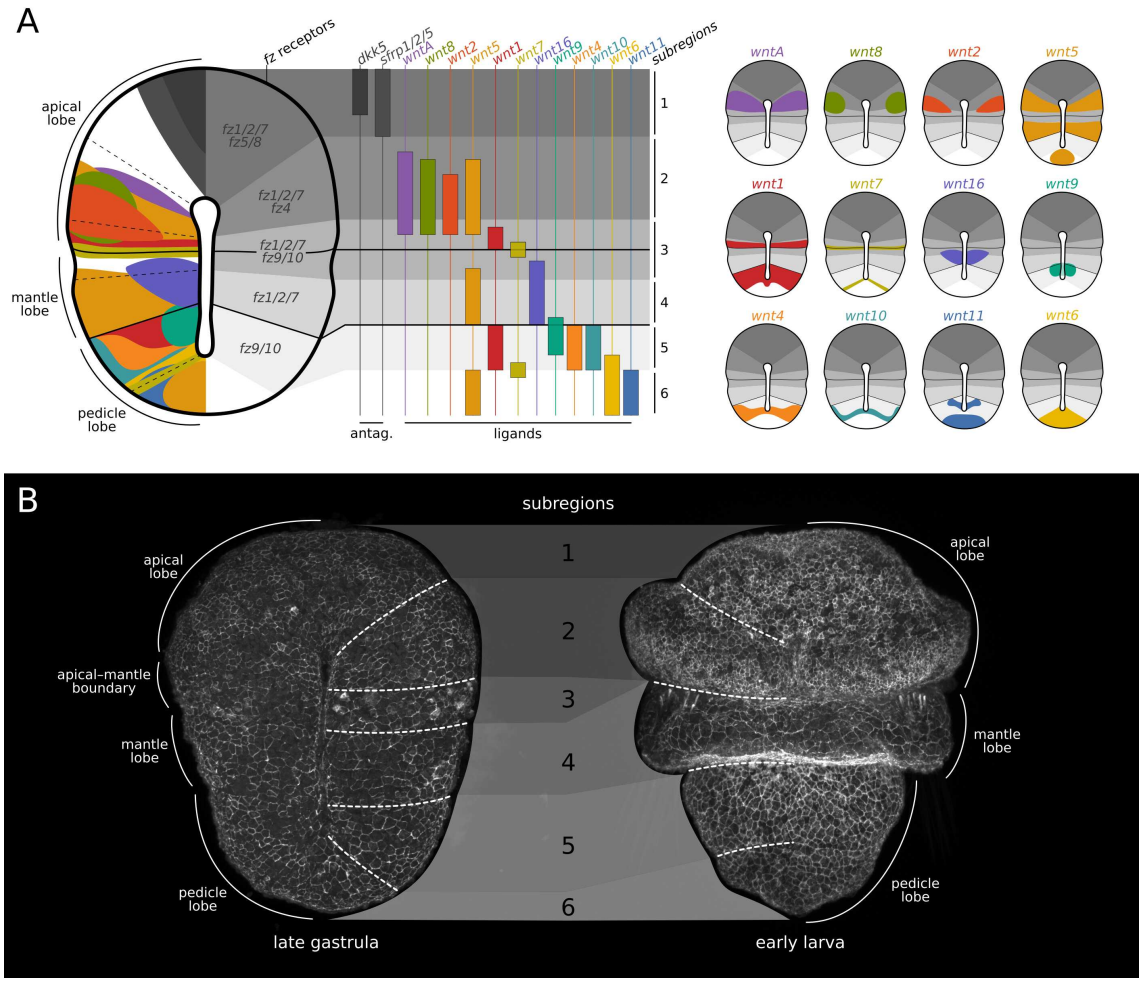

Figure 8: Summary of *Terebratalia transversa* Wnt signaling landscape. (A) Schematic drawing of a late gastrula in ventral view showing the ectodermal expression domains of Wnt, Frizzled, and antagonist genes. Wnt genes are colored by subfamilies, Frizzled genes by lighter shades of grey, and antagonists by darker shades of grey. The spatial localization of domains is superimposed on the embryo outline and projected view to highlight the different transcriptional subregions (left), and individualized for the different Wnt genes (right). (B) A late gastrula and early larva samples stained for f-actin showing the different cell shapes between the different body regions and transcriptional subregions of *T. transversa*. Solid lines represent morphological boundaries for the apical, mantle, and pedicle lobes, and dashed lines represent boundaries between transcriptional subregions.

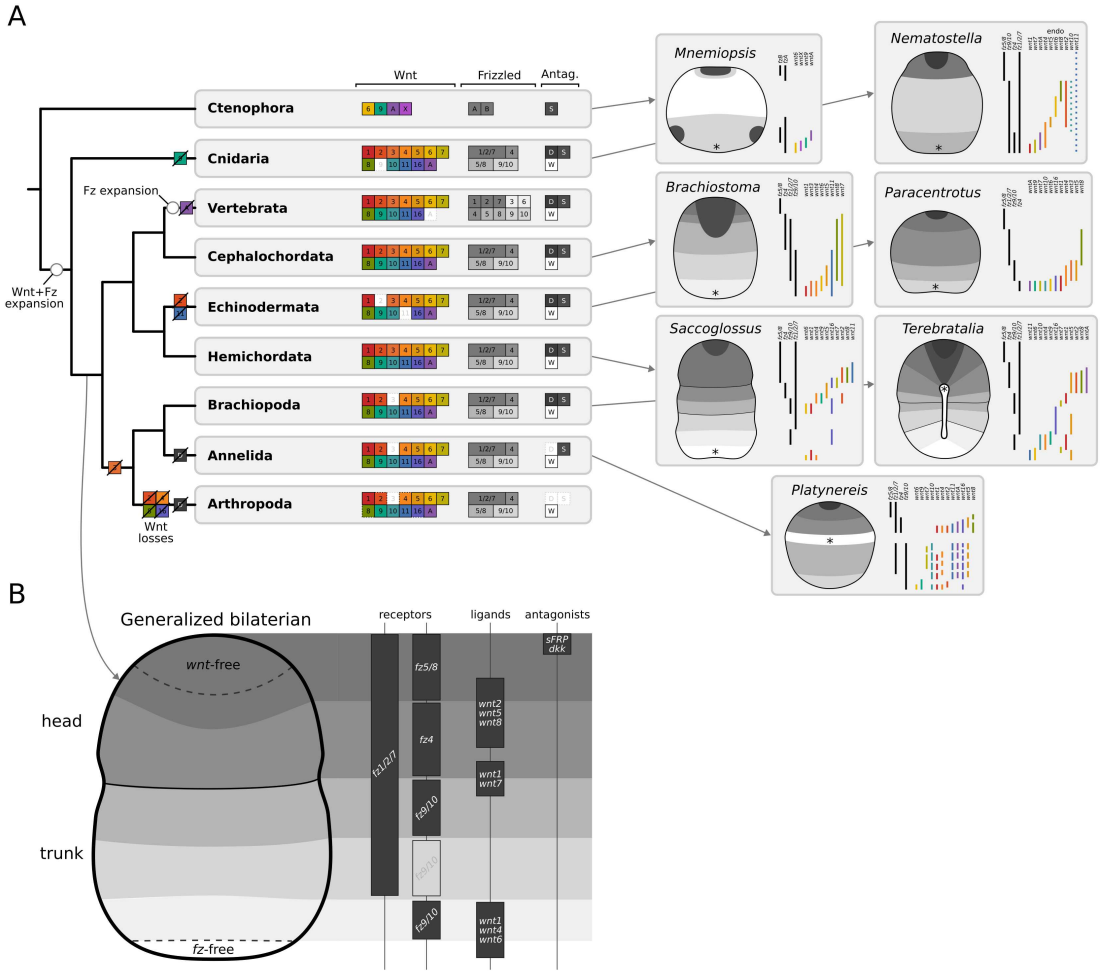

Figure 9: Comparative overview of the Wnt signaling landscape in metazoans. (A) Phylogenetic tree showing the expansion and losses of Wnt ligands, Frizzled receptors and Wnt antagonists, and the molecular repertoire of each lineage. The schematic drawings illustrate the expression of Wnt signaling components during antero-posterior patterning based on previous works on Ctenophora [103], Cnidaria [22, 105], Cephalochordata [21, 108, 109, 125–130], Echinodermata [82, 83, 106, 131–135], Hemichordata [39], Annelida [25, 38, 47, 104], and Brachiopoda [57] and this study. (B) Generalized bilaterian showing the combinations of expression domains of Wnt signaling components along the anteroposterior axis which are conserved across bilaterians. This spatial arrangement could represent the ancestral Wnt landscape in the last common ancestor of bilaterians.

Tables

Table 1: Wnt signaling transcriptional subregions in the brachiopod *Terebratalia transversa.*

Subregion	Position	Antagonists	Ligands	Receptors
1	Anterior portion of apical lobe	*dkk*, *sfrp1/2/5*	(*wnt1t*)	*fz1/2/7*, *fz5/8*
2	Posterior portion of apical lobe	-	*wntA*, *wnt8*, *wnt2*, *wnt5*	*fz1/2/7*, *fz4*
3	Boundary between apical and mantle lobes	-	*wnt1*, *wnt7*, *wnt16*	*fz1/2/7*, *fz9/10*
4	Mantle lobe	-	*wnt5*, *wnt16*	*fz1/2/7*
5	Anterior portion of pedicle lobe	-	*wnt1*, *wnt9*, *wnt11*, *wnt4*, *wnt10*, *wnt7*	*fz9/10*
6	Posterior portion of pedicle lobe	-	*wnt6*, *wnt11*, *wnt5*	-

Table 2: Maternal load of Wnt and Frizzled transcripts in metazoan eggs.

Group	Species	Wnt genes	Frizzled genes
Brachiopoda	*Terebratalia transversa*	*wnt4* and *wntA* (this study)	*fz1/2/7*, *fz5/8* and *fz4* (this study)
Brachiopoda	*Lingula anatina*	*wntA* and *wnt8* [136, 137]	*fz1/2/7*, *fz4* and *fz9/10* [136, 137]
Annelida	*Platynereis dumerilii*	No maternal Wnt transcripts [38]	*fz1/2/7* [104]
Priapulida	*Priapulus caudatus*	*wnt2*, *wnt4*, *wnt5* and *wnt8* [138]	-
Hemichordata	*Saccoglossus kowalevskii*	*wnt4* and *wnt9* [39]	*fz1/2/7* and *fz5/8* [39]
Echinodermata	*Paracentrotus lividus*	*wnt7* [106]	*fz1/2/7* and *fz5/8* [106]
Echinodermata	*Strongylocentrotus purpuratus*	*wnt6*, *wnt7* and *wnt16* [139]	*fz1/2/7* [132]
Vertebrata	*Xenopus laevis*	*wnt5*, *wnt8* and *wnt11* [140]	-
Vertebrata	*Danio rerio*	*wnt8* [141]	-
Cnidaria	*Clytia hemisphaerica*	*wnt3* [142]	*fz1* and *fz3* [142]

Table 3: Developmental stages sampled for the stage-specific transcriptome of *Terebratalia transversa*.

Stage	Time post fertilization	Description
S01	0h	oocytes
S02	8h	mid blastula
S03	19h	late blastula
S04	24h	moving late blastula
S05	26h	early gastrula
S06	37h	asymmetric gastrula
S07	51h	bilateral gastrula
S08	59h	bilobed
S09	68h	trilobed
S10	82h	early larva (first chaetae visible)
S11	98h	late larva (long chaetae, eye spots)
S12	131h	competent larva
S13	1d	juvenile
S14	2d	juvenile

Supplementary material

Figures

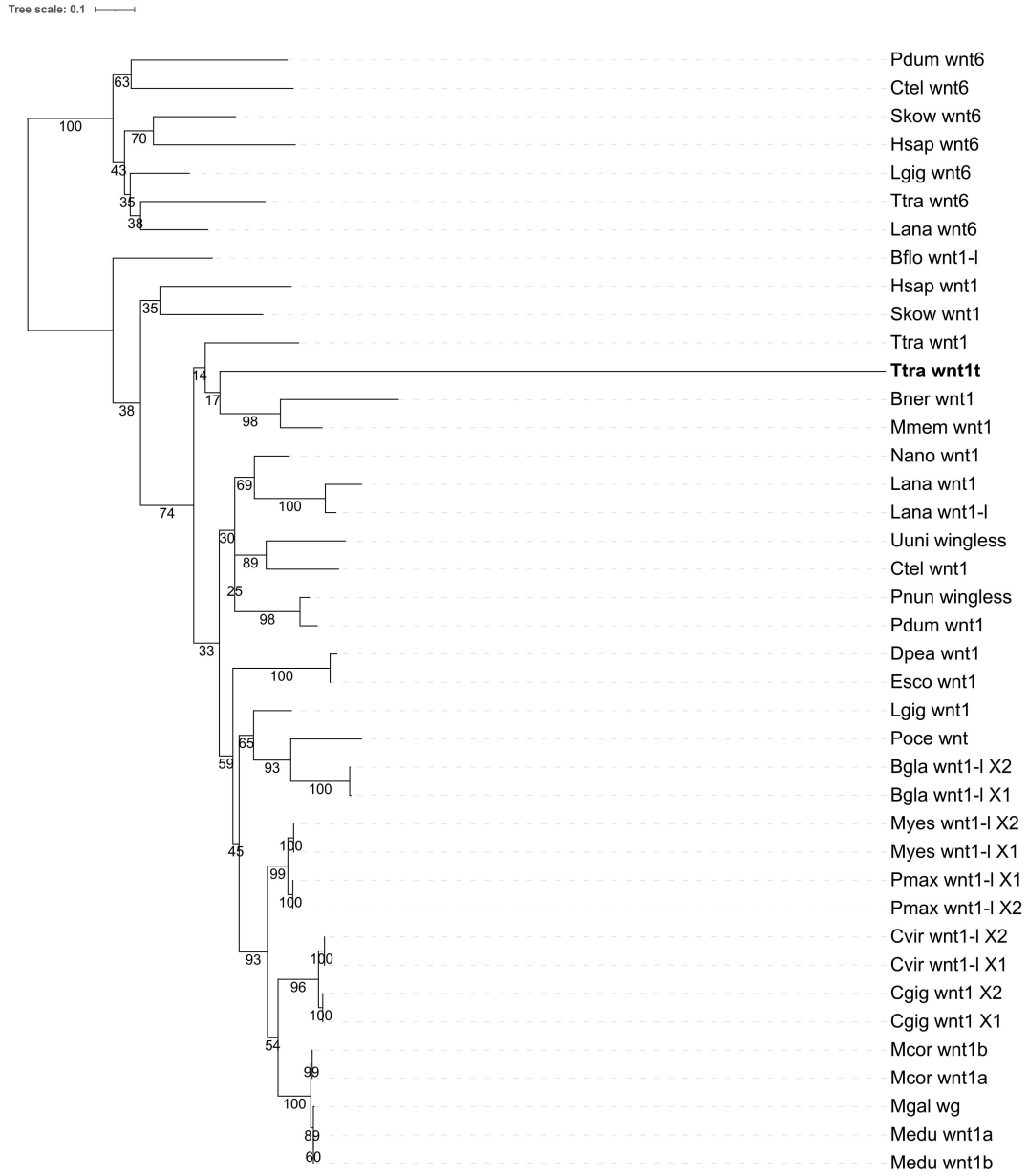

Figure S1: Phylogenetic analysis of *Terebratalia transversa* Wnt1 proteins. Best-scoring tree of a maximum likelihood phylogenetic analysis using amino acid sequences of genes from the *wnt1* subfamily with *wnt6* as an outgroup. Branch lengths are proportional to the amount of sequence change and the numbers show the support values of individual branches. Both *Terebratalia transversa* (Ttra) and *Lingula anatina* (Lana), a rhynchonelliform and a linguliform brachiopod, respectively, have two copies of *wnt1*. If this was an ancient duplication event at the base of Brachiopoda, we would expect the orthologous *wnt1* paralogs from different species to cluster together (i.e., Ttra *wnt1* with Lana *wnt1*). Instead, the tree reveals that the paralog copies of each species cluster together, suggesting that the duplication of *wnt1* occurred independently in *T. transversa* and *L. anatina*. *T. transversa wnt1t* also shows a longer branch length indicating rapid evolution. Taxon sampling was focused in spiralians. The other species are *Biomphalaria glabrata* (Bgla), *Branchiostoma floridae* (Bflo), *Bugula neritina* (Bner), *Capitella teleta* (Ctel), *Crassostrea virginica* (Cvir), *Doryteuthis pealeii* (Dpea), *Euprymna scolopes* (Esco), *Homo sapiens* (Hsap), *Lingula anatina* (Lana), *Lottia gigantea* (Lgig), *Membranipora membranacea* (Mmem), *Mizuhopecten yessoensis* (Myes), *Mytilus coruscus* (Mcor), *Mytilus edulis* (Medu), *Mytilus galloprovincialis* (Mgal), *Pecten maximus* (Pmax), *Perinereis nuntia* (Pnun), *Plakobranchus ocellatus* (Poce), *Platynereis dumerilii* (Pdum), *Saccoglossus kowalevskii* (Skow), and *Urechis unicinctus* (Uuni).

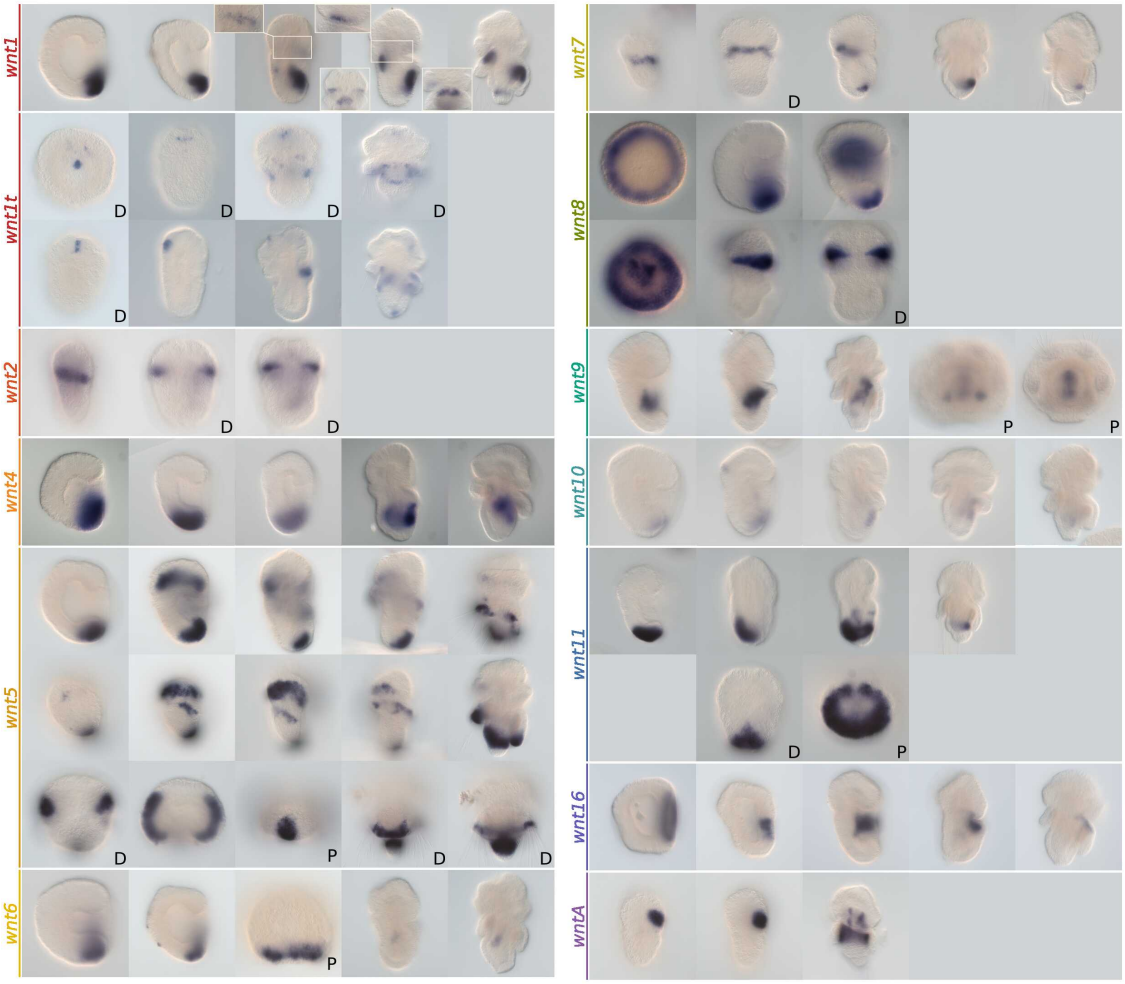

Figure S2: Whole-mount colorimetric *in situ* hybridization of *Terebratalia transversa wnt* genes. Additional lateral views of Wnt expression between early gastrula and late larva. Dorsal (D) or posterior (P) views are indicated in the respective panels.

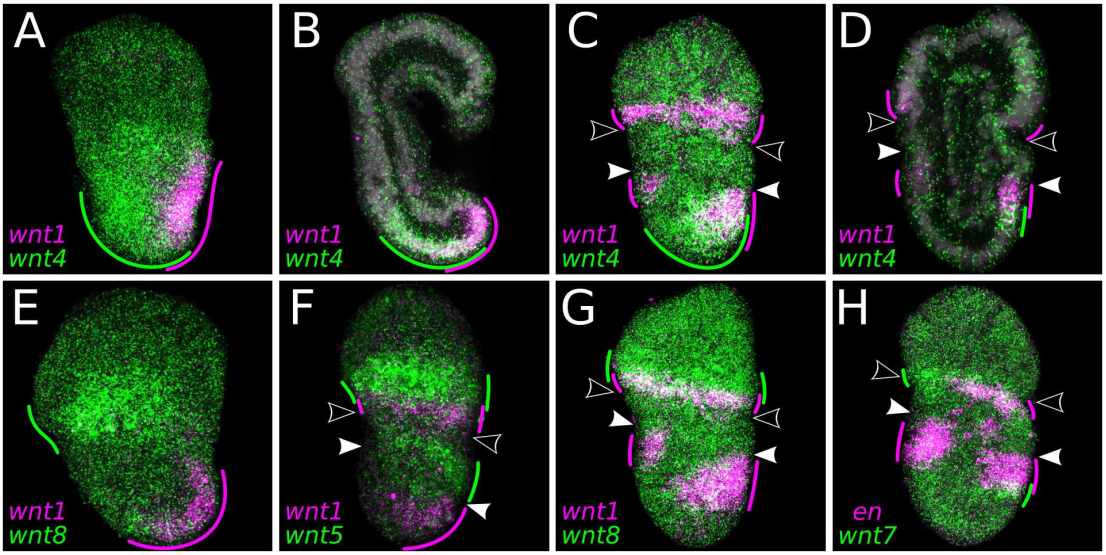

Figure S3: Whole-mount double-fluorescent *in situ* hybridization of *Terebratalia transversa wnt* genes. (A–D) Expression of *wnt1* (magenta) and *wnt4* (green) in the mid gastrula (A,B) and late gastrula (C,D). (E,G) Expression of *wnt1* (magenta) and *wnt8* (green) in the mid gastrula (E) and early larva (G). (F) Expression of *wnt1* (magenta) and *wnt5* (green) in the late gastrula. (H) Expression of *engrailed* (magenta) and *wnt7* (green) in the early larva. Green and magenta lines highlight the extension and overlap between domains. Areas in the tissue where the expression overlaps appear in white. Samples oriented with the anterior end to the top and ventral to the right (lateral views). Black arrowheads indicate the apical–mantle boundary. White arrowheads demarcate the mantle–pedicle boundary.

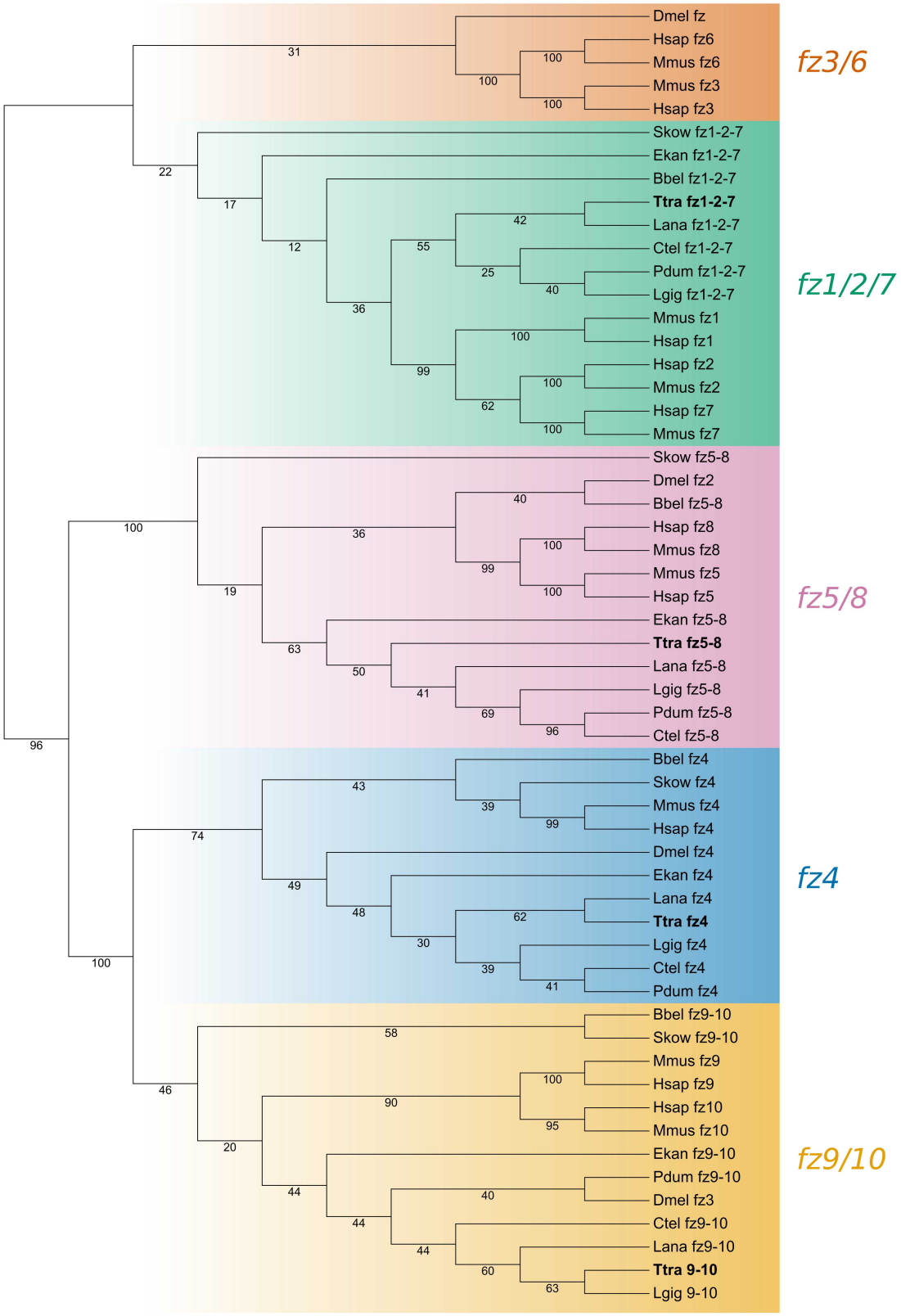

Figure S4: Orthology assignment of *Terebratalia transversa* Frizzled proteins. Best-scoring tree of a maximum likelihood phylogenetic analysis using the amino acid sequences of well-annotated Frizzled proteins. The color-coding represents different Frizzled subfamilies and the numbers show the support values of individual branches. *Terebratalia transversa* (Ttra) orthologs are highlighted in bold. The other species are *Branchiostoma belcheri* (Bbel), *Capitella teleta* (Ctel), *Drosophila melanogaster* (Dmel), *Euperipatoides kanangrensis* (Ekan), *Homo sapiens* (Hsap), *Lingula anatina* (Lana), *Lottia gigantea* (Lgig), *Mus musculus* (Mmus), *Platynereis dumerilii* (Pdum), and *Saccoglossus kowalevskii* (Skow).

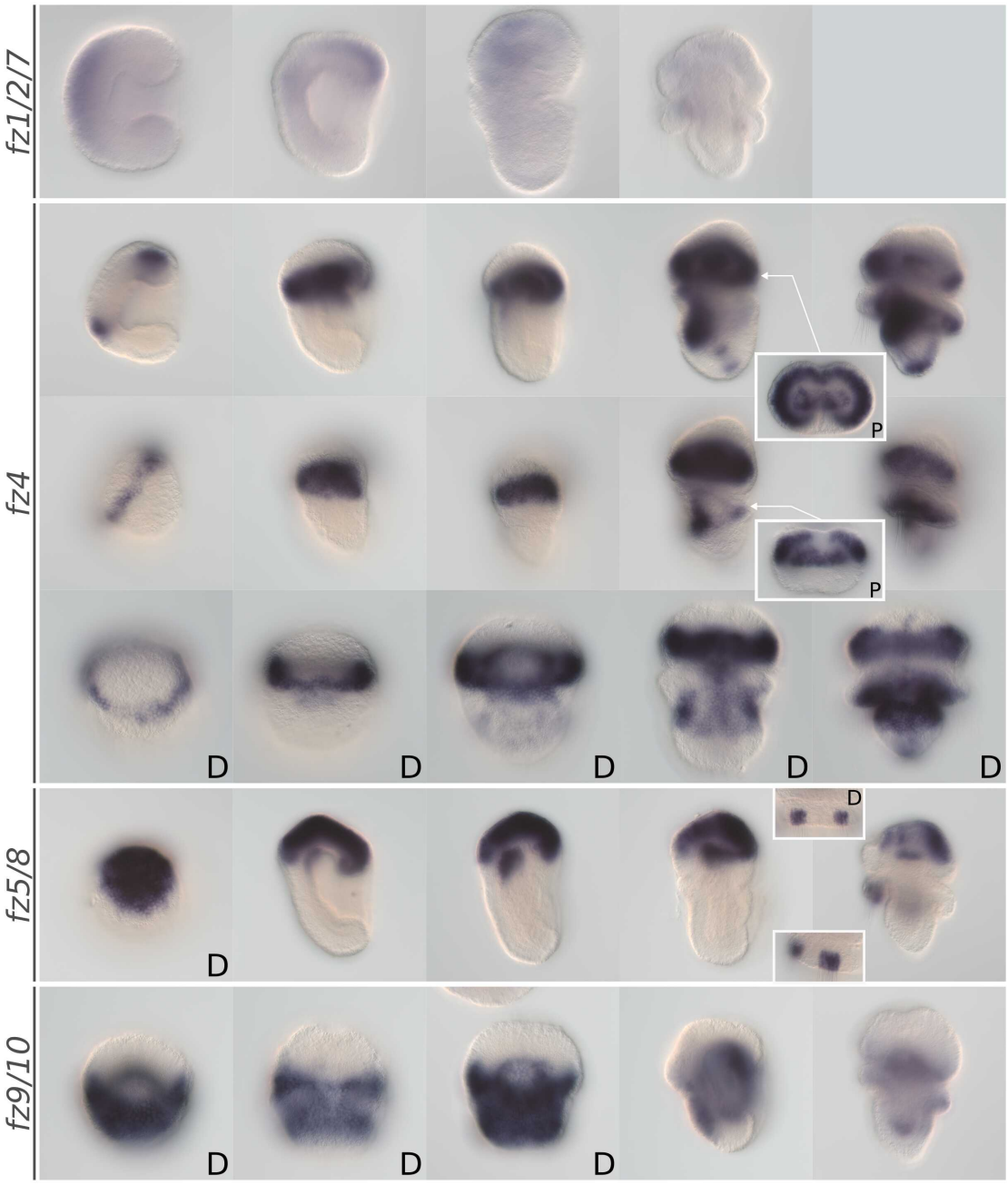

Figure S5: Whole-mount colorimetric *in situ* hybridization of *Terebratalia transversa fz* genes. Lateral, dorsal (D), and posterior (P) views between early gastrula and late larva. Samples oriented with anterior to the top and ventral to the right. In posterior views, the dorsal side to the top.

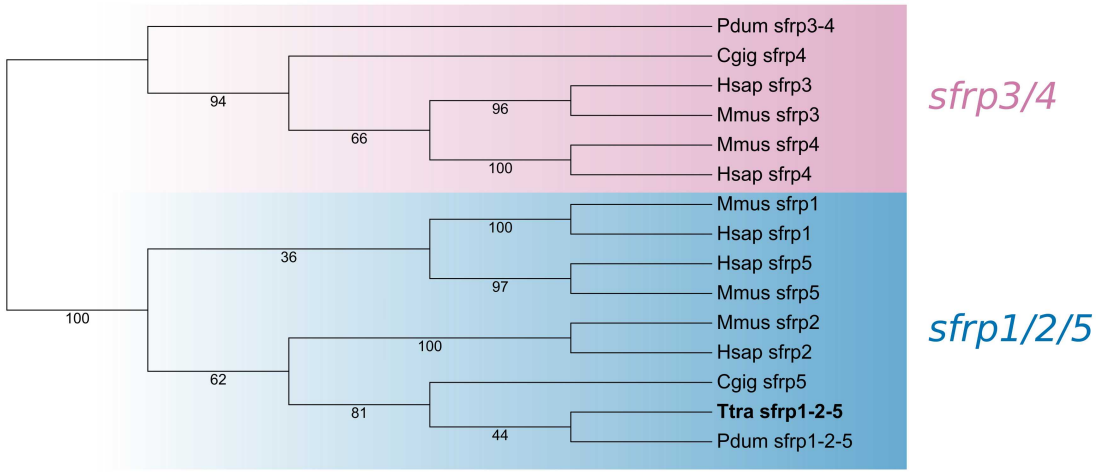

Figure S6: Orthology assignment of *Terebratalia transversa* sFRP proteins. Best-scoring tree of a maximum likelihood phylogenetic analysis using the amino acid sequences of sFRP genes. The color-coding represents different sFRP subfamilies and the numbers show the support values of individual branches. *Terebratalia transversa* (Ttra) ortholog is highlighted in bold. The other species are *Homo sapiens* (Hsap), *Crassostrea gigantea* (Cgig), *Mus musculus* (Mmus), and *Platynereis dumerilii* (Pdum).

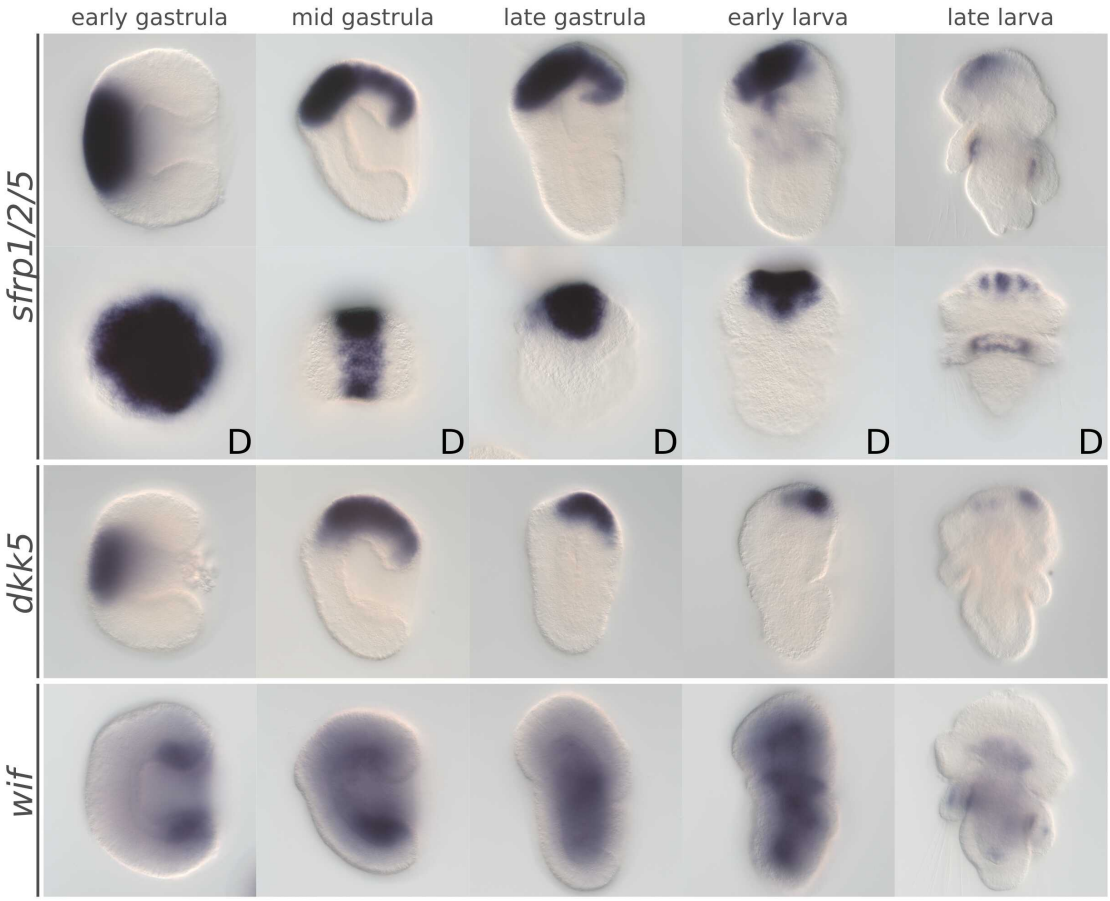

Figure S7: Whole-mount colorimetric *in situ* hybridization of *Terebratalia transversa* Wnt antagonists. Lateral views between early gastrula and late larva. Samples oriented with anterior to the top and ventral to the right. Dorsal views (D) are indicated in their respective panels.

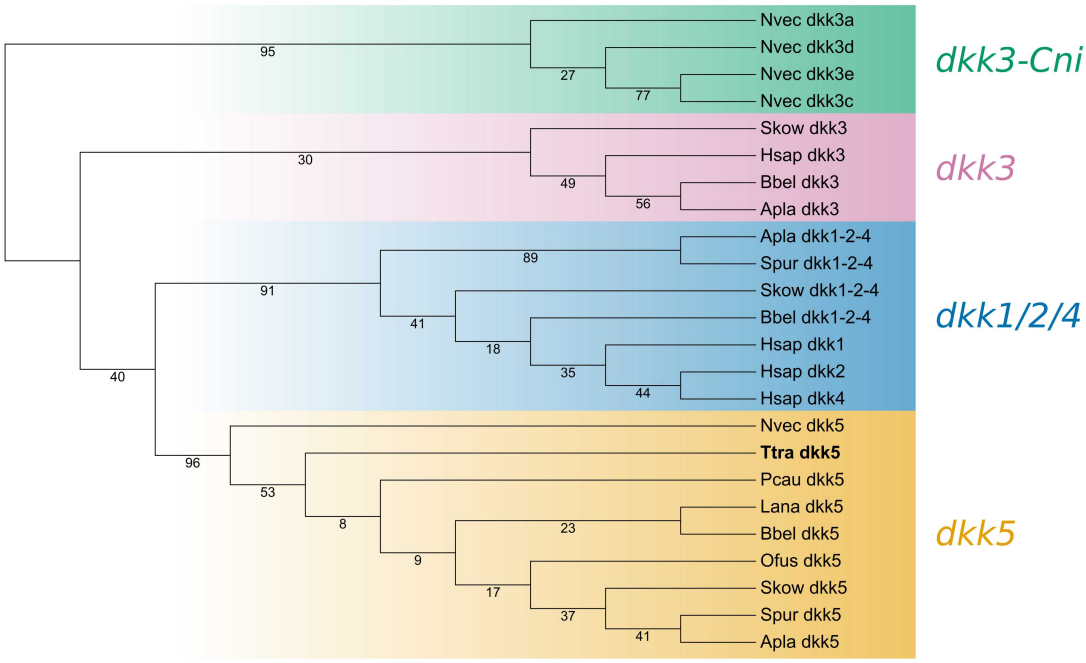

Figure S8: Orthology assignment of *Terebratalia transversa* Dkk proteins. Best-scoring tree of a maximum likelihood phylogenetic analysis using the amino acid sequences of Dkk from diverse metazoans. Color-coding represents different Dkk subfamilies. Numbers show support values of individual branches. *Terebratalia transversa* (Ttra) ortholog, highlighted in bold, groups with a previously unidentified Dkk subfamily, in addition to *dkk3* and *dkk1/2/4*, which we named *dkk5*. Non-vertebrate deuterostomes such as the hemichordate *Saccoglossus kowalevskii* (Skow), the echinoderm *Acanthaster planci* (Apla), and the cephalochordate *Branchiostoma belcheri* (Bbel), have an ortholog of each Dkk family. Vertebrates lost *dkk5*. Protostomes lost *dkk1/2/4* and *dkk3* early on, but retained *dkk5* in some lineages such as *T. transversa*, *Priapulus caudatus* (Pcau), and *Owenia fusiformis* (Ofus). Cnidarians expanded *dkk3* but lost *dkk1/2/4*. Overall, this suggests *dkk1/2/4*, *dkk3*, and *dkk5* were the ancestral subfamilies in the Cnidaria–bilaterian branch. The other species are *Homo sapiens* (Hsap), *Lingula anatina* (Lana), *Nematostella vectensis* (Nvec), and *Strongylocentrotus purpuratus* (Spur).

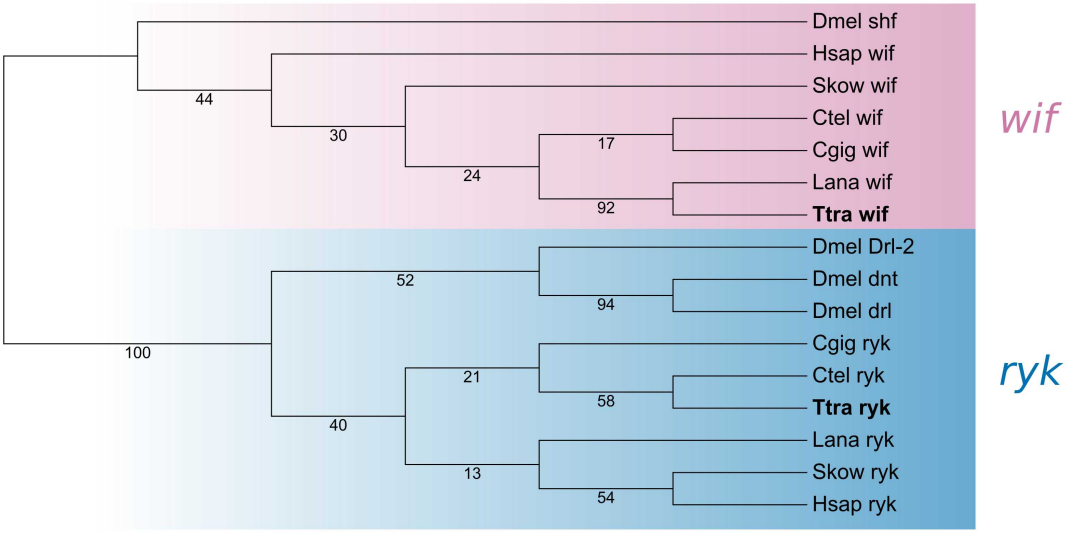

Figure S9: Orthology assignment of *Terebratalia transversa* Wif proteins. Best-scoring tree of a maximum likelihood phylogenetic analysis using the amino acid sequences of known Wif proteins (Wnt inhibitory factor). As an outgroup, we used the tyrosine-protein kinase Ryk which also has a WIF domain. The color-coding represents Wif and Ryk families. Numbers show the support values of individual branches. *Terebratalia transversa* (Ttra) orthologs are highlighted in bold. The other species are *Capitella teleta* (Ctel), *Crassostrea gigantea* (Cgig), *Drosophila melanogaster* (Dmel), *Homo sapiens* (Hsap), *Lingula anatina* (Lana), and *Saccoglossus kowalevskii* (Skow).

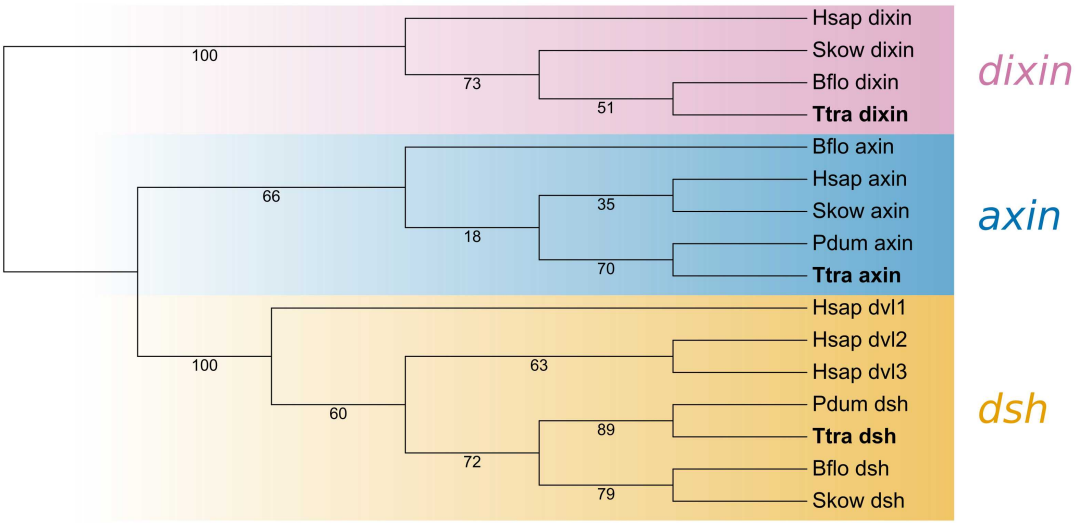

Figure S10: Orthology assignment of *Terebratalia transversa* Dsh proteins. Best-scoring tree of a maximum likelihood phylogenetic analysis using the amino acid sequences of known Dsh, Axin, and Dixin proteins. The three belong to the DIX domain superfamily. Each family is color-coded and the numbers numbers show support values of individual branches. *Terebratalia transversa* (Ttra) orthologs are highlighted in bold. The other species are *Branchiostoma floridae* (Bflo), *Homo sapiens* (Hsap), *Platynereis dumerilii* (Pdum), and *Saccoglossus kowalevskii* (Skow).

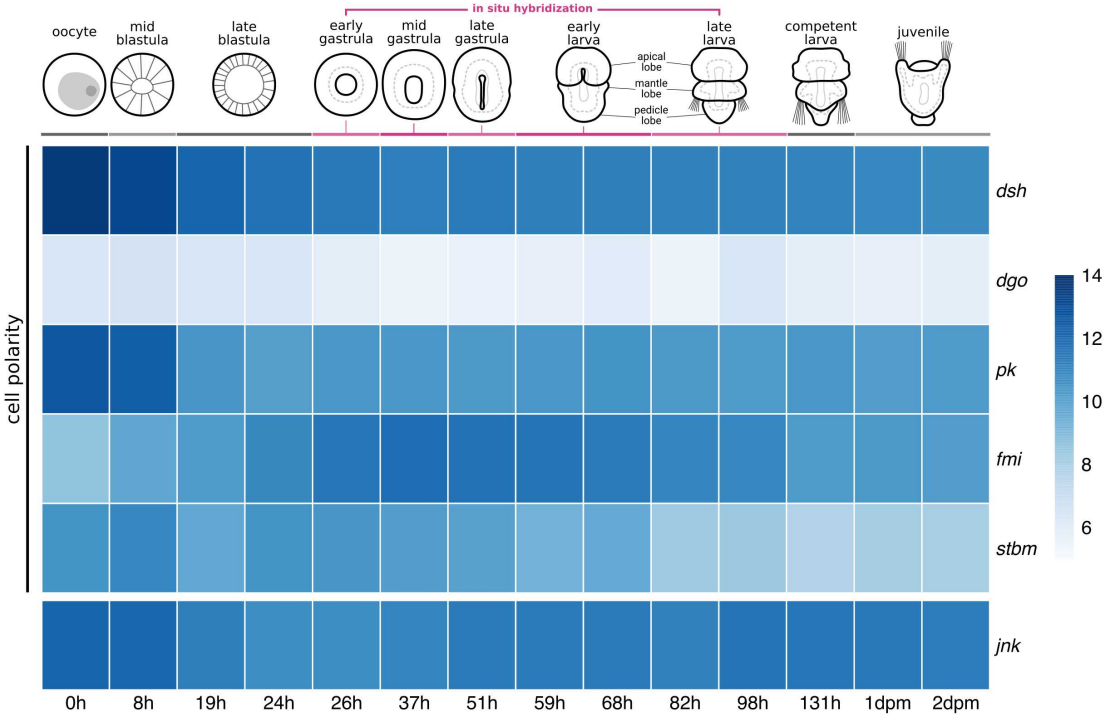

Figure S11: Expression of Wnt/PCP pathway during *Terebratalia transversa* development. The heatmap represents the log-normalized transcript counts for *dsh*, *dgo*, *pk*, *fmi*, *stbm*, and *jnk* calculated from stage-specific RNA-seq data. Each cell shows the average value between two replicates. The illustrations depict *T. transversa* developmental stages from the oocyte until the post-metamorphic juvenile. The stages we analyzed using *in situ* hybridization (early gastrula to late larva) are highlighted in magenta.

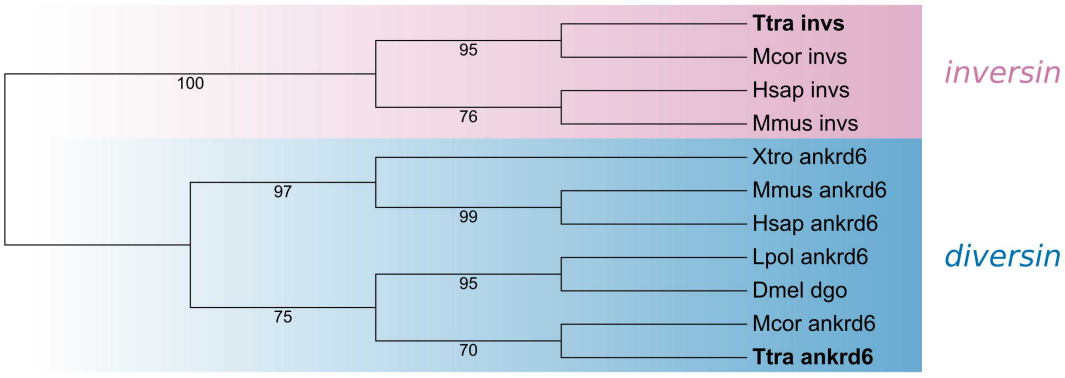

Figure S12: Orthology assignment of *Terebratalia transversa* Dgo proteins. Best-scoring tree of a maximum likelihood phylogenetic analysis using the amino acid sequences of Dgo (ANKR6 or Diversin). We used Inversin proteins as an outgroup since they also have ankyrin repeats. *Terebratalia transversa* (Ttra) orthologs are highlighted in bold. The other species are *Drosophila melanogaster* (Dmel), *Homo sapiens* (Hsap), *Limulus polyphemus* (Lpol), *Mus musculus* (Mmus), *Mytilus coruscus* (Mcor), and *Xenopus tropicalis* (Xtro).

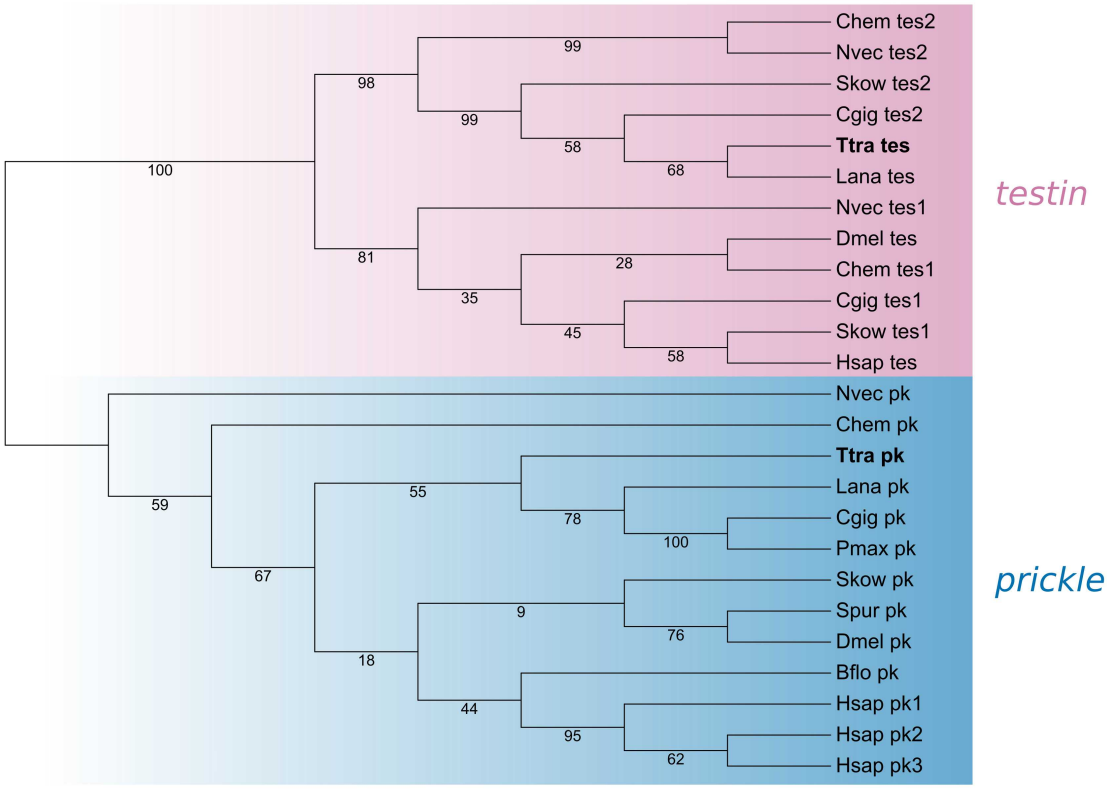

Figure S13: Orthology assignment of *Terebratalia transversa* Pk proteins. Best-scoring tree of a maximum likelihood phylogenetic analysis using the amino acid sequences of Pk from diverse metazoans. As an outgroup, we used Testin, a related protein which also contains a LIM and a PET domain. *Terebratalia transversa* (Ttra) orthologs are highlighted in bold. The other species are *Clytia hemisphaerica* (Chem), *Crassostrea gigantea* (Cgig), *Drosophila melanogaster* (Dmel), *Homo sapiens* (Hsap), *Lingula anatina* (Lana), *Nematostella vectensis* (Nvec), *Pecten maximus* (Pmax), and *Saccoglossus kowalevskii* (Skow).

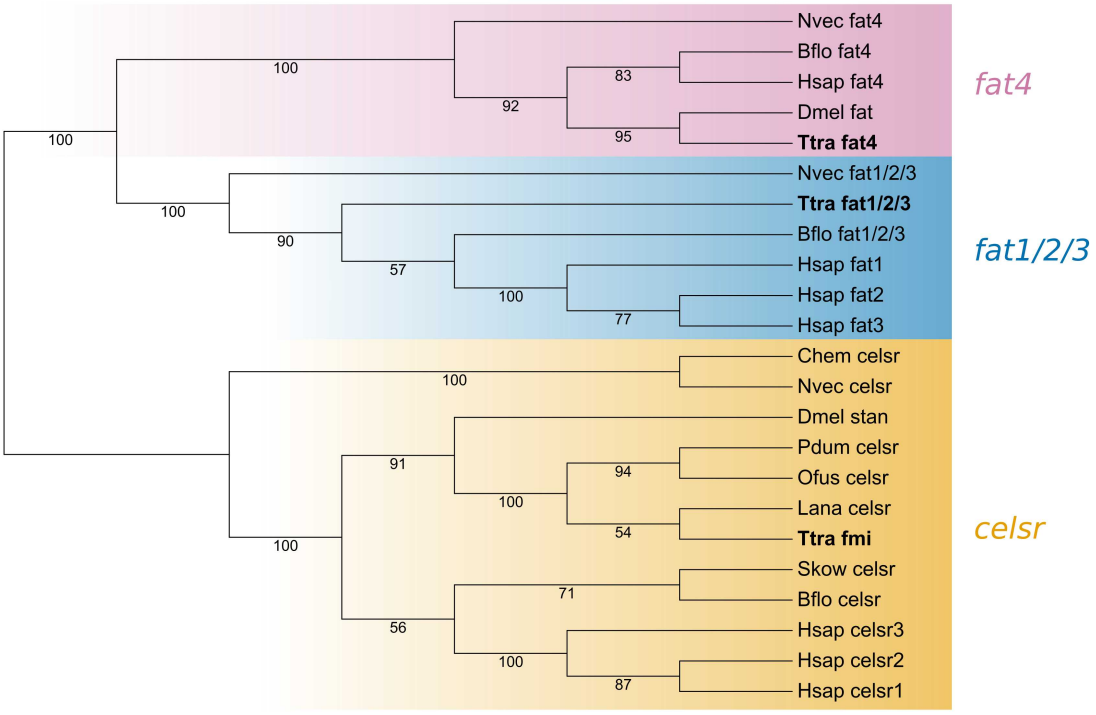

Figure S14: Orthology assignment of *Terebratalia transversa* Fmi proteins. Best-scoring tree of a maximum likelihood phylogenetic analysis using the amino acid sequences of Fmi. As outgroups, we used the related Fat family protocadherins which also contain cadherin and laminin domains. *Terebratalia transversa* (Ttra) orthologs are highlighted in bold. The other species are *Branchiostoma floridae* (Bflo), *Clytia hemisphaerica* (Chem), *Drosophila melanogaster* (Dmel), *Homo sapiens* (Hsap), *Lingula anatina* (Lana), *Nematostella vectensis* (Nvec), *Owenia fusiformis* (Ofus), *Platynereis dumerilii* (Pdum), and *Saccoglossus kowalevskii* (Skow).

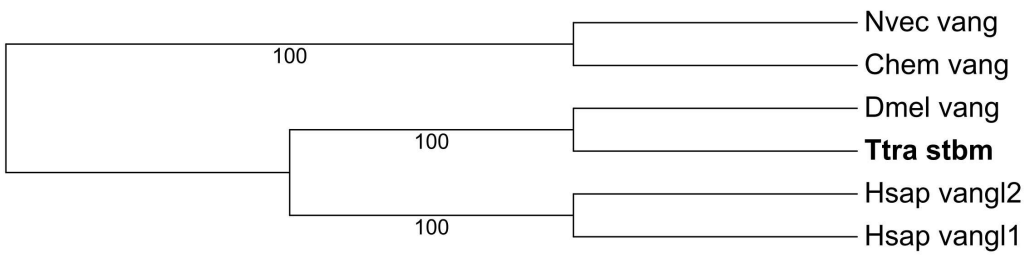

Figure S15: Orthology assignment of *Terebratalia transversa* Stbm proteins. Best-scoring tree of a maximum likelihood phylogenetic analysis using the amino acid sequences of Stbm from selected metazoans. *Terebratalia transversa* (Ttra) ortholog is highlighted in bold. The other species are *Clytia hemisphaerica* (Chem), *Drosophila melanogaster* (Dmel), *Homo sapiens* (Hsap), and *Nematostella vectensis* (Nvec).

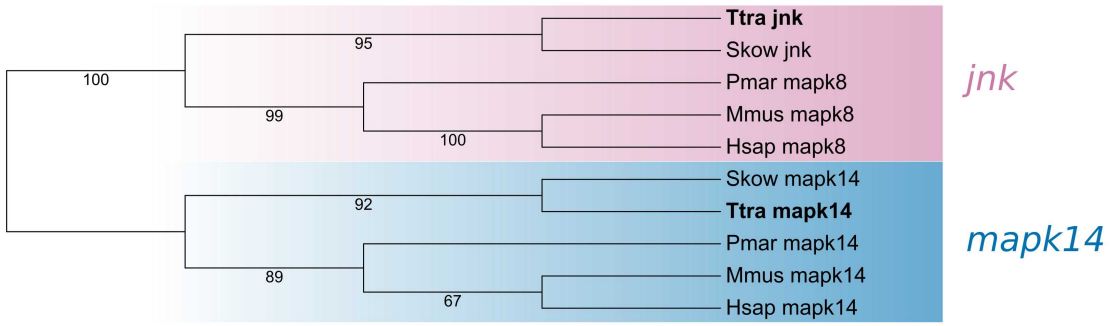

Figure S16: Orthology assignment of *Terebratalia transversa* Jnk proteins. Best-scoring tree of a maximum likelihood phylogenetic analysis using the amino acid sequences of Jnk. As outgroup, we used the related protein Mapk14. *Terebratalia transversa* (Ttra) orthologs are highlighted in bold. The other species are *Homo sapiens* (Hsap), *Mus musculus* (Mmus), *Petromyzon marinus* (Pmar), and *Saccoglossus kowalevskii* (Skow).

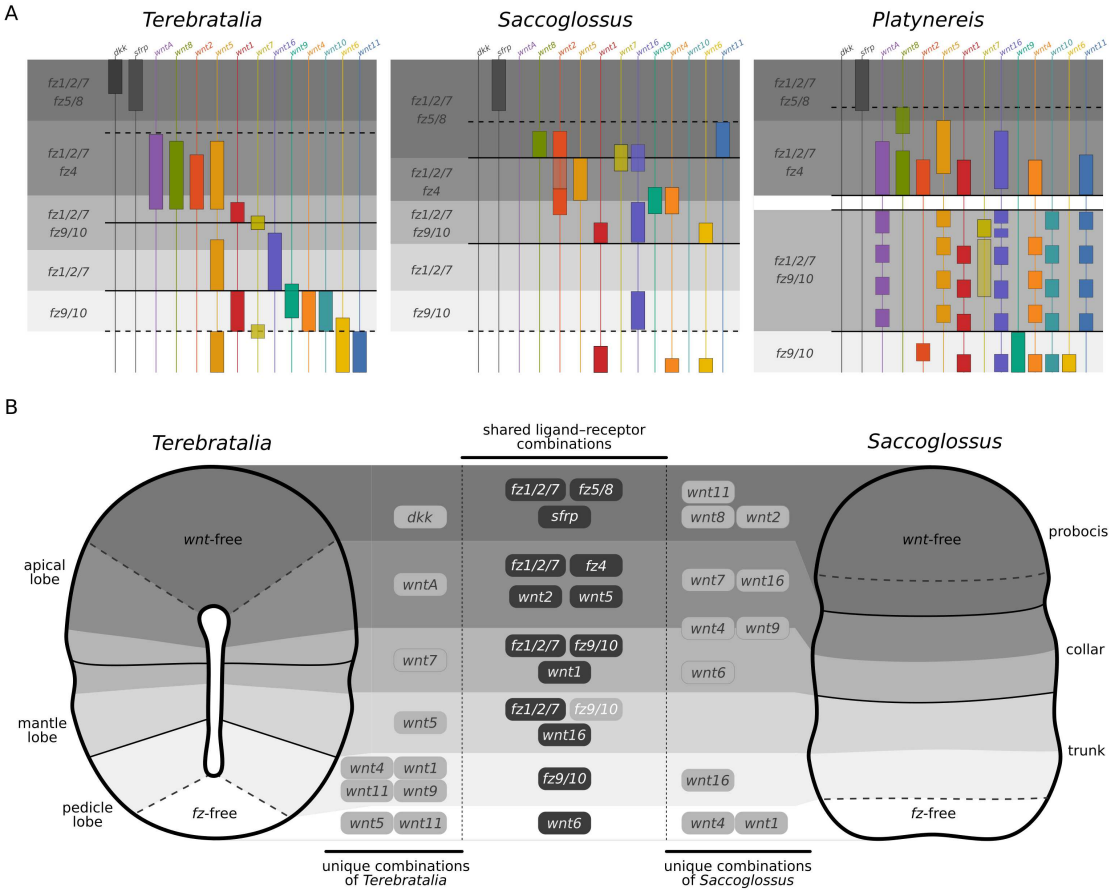

Figure S17: Wnt signaling ligand–receptor contexts of *Terebratalia transversa* compared to other animals. (A) Spatial localization of *wnt* ligands, *fz* receptors, and *dkk*/*sfrp* antagonists highlighting the transcriptional subregions of *Terebratalia* (brachiopod), *Saccoglossus* (hemichordate), and *Platynereis* (annelid). Wnt genes are colored by subfamilies, Frizzled genes by lighter shades of grey, and Wnt antagonists by darker shades of grey. (B) Detailed comparison of shared and different unique combinations of Wnt signaling components between a brachiopod and an hemichordate. Solid lines represent morphological boundaries for the apical, mantle, and pedicle lobes, and dashed lines represent boundaries between transcriptional subregions.